# Comprehensive Automobile Research System (CARS) – a Python-based Automobile Emissions Inventory Model

Bok H. Baek[1], Rizzieri Pedruzzi[2], Minwoo Park[3], Chi-Tsan Wang[1], Younha Kim[4], Chul-Han Song[5], and Jung-Hun Woo[3,6]

[1]Center for Spatial Information Science and Systems – George Mason University, Fairfax, VA, USA.

[2]Department of Sanitary and Environmental Engineering, Federal University of Minas Gerais, Belo Horizonte, Brazil.

[3]Department of Technology Fusion Engineering, College of Engineering, Konkuk University, Seoul, Republic of Korea

[4]Energy, Climate, and Environment program, International Institute for Applied Systems Analysis, Laxenburg, Austria

[5]School of Earth and Environmental Engineering, Gwangju Institute Science and Technology, Gwangju, Republic of Korea

[6]Civil and Environmental Engineering, College of Engineering, Konkuk University, Seoul, Republic of Korea

*corresponding to: Jung-Hun Woo* (jwoo@konkuk.ac.kr)

## Abstract

The Comprehensive Automobile Research System (CARS) is an open-source python-based automobile emissions inventory model designed to efficiently estimate high quality emissions from motor-vehicle emission sources. It can estimate the criteria air pollutants, greenhouse gases, and air toxins in any spatial resolution based on the spatiotemporal resolutions of input datasets. The CARS is designed to utilize local vehicle activity data, such as vehicle travel distance, road link-level network Geographic Information System (GIS) information, and vehicle-specific average speed by road type, to generate an automobile emissions inventory for policymakers, stakeholders, and the air quality modeling community. The CARS model adopted the European Environment Agency's (EEA) onroad automobile emissions calculation methodologies to estimate the hot exhaust, cold start, and evaporative emissions from onroad automobile sources. It can optionally utilize average speed distribution (ASD) of all road types to reflect more realistic vehicle speed variations. Also, through utilizing high-resolution road GIS data, the CARS can estimate the road link-level emissions to improve the inventory's spatial resolution. When we compared the official 2015 national mobile emissions from Korea's Clean Air Policy Support System (CAPSS) against the ones estimated by the CARS, there is a significant increase in volatile

33 organic compounds (VOCs) (33%) and carbon monoxide (CO) (52%) measured, with a slight
34 increase in fine particulate matter (PM$_{2.5}$) (15%) emissions. Nitrogen oxides (NOx) and sulfur
35 oxides (SOx) measurements are reduced by 24% and 17% respectively in the CARS estimates.
36 The main differences are driven by different vehicle activities and the incorporation of road-
37 specific ASD, which plays a critical role in hot exhaust emission estimates but wasn't implemented
38 in Korea's CAPSS mobile emissions inventory. While 52% of vehicles use gasoline fuel and 35%
39 use diesel, gasoline vehicles only contribute 7.7% of total NOx emissions while diesel vehicles
40 contribute 85.3%. But for VOC emissions, gasoline vehicles contribute 52.1% while diesel
41 vehicles are limited to 23%. Diesel buses comprise of only 0.3% of vehicles and has the largest
42 contribution to NO$_x$ emissions (8.51% of NO$_x$ total) per vehicle due to having longest daily vehicle
43 kilometer travel (VKT). For VOC emissions, Compressed Natural Gas (CNG) buses are the largest
44 contributor at 19.5% of total VOC emissions. For primary PM$_{2.5}$, more than 98.5% is from diesel
45 vehicles. The CARS model's in-depth analysis feature can assist government policymakers and
46 stakeholders in developing the best emission abatement strategies.

47 Keywords: inventory: automobile, vehicle emissions, hot exhaust, cold start, evaporative, python


# 1   Introduction

49      Globally, ambient pollution causes more than 4.2 million premature deaths every year
50 (Cohen et al., 2017), and Burnett et al. (2018) estimated the health burden is closer to 9 million
51 deaths from ambient PM concentrations. To effectively mitigate air pollutants, governments have
52 been implementing stringent air pollution control policies to reduce harmful regional air pollutants
53 (Hogrefe et al., 2001a; Hogrefe et al., 2001b; Dennis et al., 2010; Rao et al., 2011; Appel et al.,
54 2013; Luo et al., 2019). The chemical transport model (CTM) simulation results strongly rely on
55 precise input data, such as emission inventory, meteorology, land surface parameters, and chemical
56 mechanisms in the atmosphere.

57      The transportation sector is one of the major anthropogenic emissions in urban areas. The
58 tailpipe emissions from the vehicle's combustion process contain many air pollutants, including
59 nitrogen oxides (NOx), volatile organic compounds (VOCs), carbon monoxide (CO), ammonia
60 (NH$_3$), sulfur dioxide (SO$_2$), and primary particulate matter (PM) which participates in the
61 formation of detrimental secondary pollutants like ozone and PM$_{2.5}$ in the atmosphere. In the Seoul
62 Metropolitan Area (SMA) in South Korea, transportation automobile sources contribute the most
63 to the total NO$_X$ and primary PM$_{2.5}$ emissions across all emission sources (Choi et al., 2014; Kim
64 et al., 2017a; Kim et al., 2017b; Kim et al., 2017c). Thus, it is critical to understand and better
65 represent the emission patterns from transportation automobile sources in the CTM model. The
66 use of process-based automobile emission models is highly recommended to meet the needs in

67  CTM model because it can estimate high resolution spatiotemporal automobile emissions
68  (Moussiopoulos et al., 2009; Russell and Dennis, 2000).

69      There are two methodologies known in emission inventory development: top-down and
70  bottom-up. The choice of methods is determined by the input data availability. The top-down
71  approach primarily relies on the aggregated and generalized country or regional information,  and
72  is typically used in developing countries where only limited datasets and information are available.
73  It has its limitations on representing the vehicle emission process realistically due to the lack of
74  detailed activity and ancillary supporting data. However, the bottom-up approach requires higher
75  quality spatiotemporal activity datasets like road network information, vehicle composition
76  (vehicle type, engine size, vehicle age, and fuel-technology), pollutant-specific emissions factors,
77  road segment length, traffic activity data, and fuel consumption (EEA, 2019; Ibarra-Espinosa et
78  al., 2018b; IEMA, 2017). It can generate more accurate and detailed automobile emissions across
79  various operating processes, such as hot exhaust, evaporative, idling, and hot soak (Nagpure et al.,
80  2016; Ibarra-Espinosa et al., 2018a).

81      There are several bottom-up mobile emissions models available, like MOVES (MOtor
82  Vehicle Emissions Simulator) from the U.S. Environmental Protection Agency (USEPA), the
83  European Environment Agency's (EEA) model COPERT (COmputer Programmed to calculate
84  Emissions from Road Transport), the HERMES (High-Elective Resolution Modelling Emission
85  System) from Barcelona Supercomputing Center (Guevara et al., 2019), the VEIN (Vehicular
86  Emissions INventory) model developed by Ibarra-Espinosa et al. (2017), and the VAPI (Vehicular
87  Air Pollution Inventory) model developed by Nagpure and Gurjar (2012) for India (Nagpure et al.,
88  2016). While these models are all bottom-up emission inventory models, a single model cannot
89  meet all modelers, policymakers, and stakeholders' needs because each model holds its own pros
90  and cons. They are developed differently to meet specific user needs based on the types of traffic
91  activity and emission factors, emission calculation methodologies, and other traffic related inputs
92  such as average speed distribution and geographical resolution. Each model is developed with
93  different levels of specificity, underlying data sets, and modeling assumptions.

94      The MOVES model has the ability to generate high quality emissions for up to 16 different
95  emission processes (i.e., Running Exhaust, Start Exhaust, Evaporative, Refueling, Extended Idling,
96  Brake, Tire, etc.). It can simulate not only county-level but also road segment level emissions
97  depending on data availability. It can also reflect local meteorological conditions, such as ambient
98  temperature and relative humidity, which can significantly impact both pollutants and emissions
99  processes (Choi et al., 2017; Perugu et al., 2018). One major disadvantage of this model is that it
100 is difficult to update and apply to countries outside of the U.S. because it has a high degree of
101 specificity. The COPERT model, widely used in European countries,  can model emissions in high
102 resolution, is fully integrated with the EEA's onroad vehicle emissions factors guidelines, and can
103 generate a complete quality assurance (QA) and visualization summary (Ntziachristos et al., 2009).
104 The cons are that it is a proprietary commercial licensed software, limited to EEA guidance, and

105 challenging to modify and update with any key input datasets like the latest emission factors from
106 non-European countries (Lejri et al., 2018; Rey DR, 2021; Li et al., 2019; Lv et al., 2019; Smit et
107 al., 2019).

108 The HERMES and VEIN are both recently released bottom-up inventory models. They
109 have their pros in that they are both open-source models based on open-source computing
110 languages (Python and R), which provide transparency of the emission calculations with a
111 considerable amount of data behind them (Ibarra-Espinosa et al., 2018b; Guevara et al., 2019).
112 Both models are driven by comma-separated value (CSV) formatted input files, making it very
113 easy for users to modify the input datasets. They are also based on the EEA's emission calculation
114 method and equipped with a complete QA and visualization tool based on Python and R libraries.
115 However, it is not an easy task to develop the emission factors, and other required input datasets
116 for other countries and implement any control strategy plan feature to generate a responsive
117 reduced emissions inventory.

118 Overall, there are multiple shortcomings in incorporating these bottom-up models into
119 CTM studies. They require strong programming skills to operate, such as collecting and preparing
120 the input data to fit the model requirements, configuring the model variables, and changing specific
121 variables that may be embedded in the code. Another downside is that while the geographical
122 administration-level (e.g., county level) emissions inventory can be estimated by these models, it
123 requires a 3rd party emissions processor like the SMOKE (Sparse Matrix Operator Kerner
124 Emissions) modeling system (Baek and Seppanen, 2021) to process and generate spatially and
125 temporally resolved emissions inputs for CTM. Some detailed information, like link-level hourly
126 driving patterns, can be lost in the emissions processing steps.

127 There is no single model capable of meeting all the requirements across various spatial and
128 temporal scales (Pinto et al., 2020). However, transparency, simplicity, and a user-friendly
129 interface are requirements for those who mainly work in transportation policy and air quality
130 modeling development (Fallahshorshani et al., 2012; Kaewunruen et al., 2016; Sallis et al., 2016;
131 Sun et al., 2016; Tominaga and Stathopoulos, 2016). Thus, the ideal motor vehicle emissions
132 modeling system would be computationally optimized, easy-to-use, and has a user-friendly
133 interface. Additionally, the model should easily adapt detailed local activity information and the
134 state-of-art emission factors as inputs to represent them in the highest resolution possible
135 temporally and spatially.

136 We have developed the Comprehensive Automobile Research System (CARS) to meet these
137 requirements, especially for the air quality research community, policymakers, and air quality
138 modelers. The CARS is a stand-alone, fully modularized, computationally optimized, python-
139 based automobile emission model. The modularization improves the efficiency of processing times
140 as once district and road link-level annual/monthly/daily total emissions are computed; the rest of
141 the processes are optional. It can generate chemically speciated, spatially gridded, hourly

142 emissions for CTMs without any 3$^{rd}$ party programs to develop the highest quality CTM-ready
143 emissions inputs. Details on modularization will be discussed later. The CARS model can be easily
144 adopted and is simple for users to add new functions or modules in the future. The application of
145 the CARS to South Korea will be described in detail later.

## 2 CARS Emissions Calculation

147     The CARS is an open-source Python-based customizable motor vehicle emissions
148 processor that estimates onroad and offroad emissions for specific criteria and toxic air pollutants.
149 Figure 1 is a schematic of the CARS overview. It applies vehicle, engine, and fuel specific
150 emission factors to traffic data to estimate the local level annual, monthly, and daily total emissions
151 inventory. The emissions inventory calculations require a list of pollutant-specific emissions
152 factors by vehicle age, local activity data, average speed profile/distribution by road type, and
153 geographic information system (GIS) road segment shapefiles inputs. The spatial resolution of
154 vehicle kilometer travel (VKT) determines the CARS geographic scale (i.e. district, county, state,
155 and country) for emission calculations. Unlike the district-level Korea Clean Air Policy Support
156 System (CAPSS) automobile emission inventory (Lee et al., 2011a; Lee et al., 2011b), the CARS
157 applies high resolution annual average daily traffic (AADT) data from the road GIS shapefiles to
158 distribute the total district emissions into road link-level emissions. Optionally, these road link-
159 level emissions can be used to generate spatially gridded CTM-ready emissions input data once
160 the output modeling domain is defined. The summary of input files by categories are presented in
161 Appendix H. How the CARS estimates spatially and temporally enhanced automobile emissions
162 inventories will be discussed in detail next chapter.

163     South Korean traffic databases from the Korea National Institute of Environmental
164 Research (NIER) CAPSS team (Lee et al., 2011b) were used in this study to compute the updated
165 onroad automobile emissions inventory. The databases include individual vehicle activity data
166 (daily total VKT), road activity data (average speed distribution by road), vehicle age specific
167 emission factors, road type information, surface weather data, and GIS road shapefiles.

### 2.1 Individual Daily Average VKT Activity Data

169     The individual vehicle VKT data is used to reflect human activity. This study imported the
170 national registered vehicle-specific daily total VKT from South Korea's Vehicle Inspection
171 Management System (VIMS), which belongs to the Korea Transportation Safety Authority
172 (KTSA). It contains over 50 million records of vehicle-specific daily total VKT from 2013 to 2017.
173 For the CARS model, we first sorted these records by the vehicle identification number (VIN) to
174 remove any duplicates and then built vehicle-specific daily total VKT traffic activity data in the
175 CSV format. The summary of those vehicle numbers and VKTs is presented in Fig. 2. Sedan
176 vehicles using gasoline fuel comprise the greatest percentage of total vehicles at 47% (~10.4

177    million) and have the highest VKT. While most vehicles demonstrate a paired pattern between the
178    number of vehicles and daily VKT, LPG (liquefied petroleum gas)-fueled taxi shows high VKT
179    with low vehicle numbers due to their long distance travel daily patterns.

180        The VIN ($vin$) information is used to calculate vehicle-specific daily average VKT ($VKT_{vin}$,
181    km d$^{-1}$). In Eq. (1), the individual daily average vehicle VKT ($VKT_{vin}$) is calculated based on the
182    cumulative mileage ($M_{f;vin}$) between the last inspection date ($D_{f;vin}$) and registration date ($D_{0;vin}$).
183    Each vehicle is categorized with Korea's NIER based on a combination of vehicle types (e.g.,
184    sedan, truck, bus, etc), engine sizes (e.g., compact, full size, midsize, etc), and fuel types (e.g.,
185    gasoline, diesel, LPG, etc). Full details of vehicle types and daily total VKT are shown in Appendix
186    A and B.

187
$$VKT_{vin} = \frac{M_{f;vin}}{D_{f;vin} - D_{0;vin}} \qquad (1)$$

188    **2.2    Emission Calculations**

189        Automobile emission sources include motorized engine sources on the paved road network
190    and off the road network (e.g., driveway and parking lots). The CARS model doesn't currently
191    simulate emissions from nonroad emission sources, such as aviation, railways, construction,
192    agricultures, lawn mowers, and boats. The CARS model simulates the onroad automobile
193    emissions from network roads using their local traffic-related datasets. The following section
194    explains the approach of the onroad automobile emission processes. The onroad emission ($E_{onroad}$)
195    in the CARS is defined in Eq. (2), which includes three major emission processes (Ntziachristos
196    and Samaras, 2000):

197
$$E_{onroad} = E_{hot} + E_{cold} + E_{vap} \qquad (2)$$

198    The hot exhaust emissions ($E_{hot}$) are the vehicle's tailpipe emissions when the internal combustion
199    engine (ICE) combusts the fuel to generate energy under the average operating temperature. The
200    cold start emissions ($E_{cold}$) are the tailpipe emissions from the ICE when the cold vehicle engine is
201    ignited and the operational temperature is below average condition. The evaporative VOC
202    emissions ($E_{vap}$) are the emissions evaporated/permeated from the fuel systems (fuel tanks,
203    injection systems, and fuel lines) of vehicles.

204        The CARS first applies the hot exhaust emission factors by vehicle type, age, fuel, engine,
205    and pollutants to individual daily total VKT to compute the hot exhaust emissions. The rest of the
206    processes for cold start and evaporative emissions are calculated afterwards. The emission
207    calculation methodologies used in the CARS model are based on tier 2 and tier 3 methodologies
208    from the EEA's mobile emission inventory guidebook (EEA, 2019) to be consistent with Korea's
209    National Emission Inventory System (NEIS) (Lee et al., 2011a).

### 2.2.1 Hot Exhaust Emissions

Hot exhaust emissions is the exhaust gas from the combustion process in an ICE. The ICE combustion cycle generally causes incomplete combustion processes which emit hydrocarbons, carbon monoxide (CO), and particulate matter (PM). These are not completely controlled by the after-treatment equipment, such as a three-way catalytic converter, and released into the atmosphere. The sulfur compounds in the fuel are oxidized and become sulfur oxides ($SO_x$). Nitrogen oxides ($NO_x$) are produced due to the abundance of nitrogen ($N_2$) and oxygen ($O_2$) during the combustion process.

Equation 3 represents the calculation of daily individual vehicle hot exhaust emission rate, $E_{hot; p,vin,myr}$ (g d$^{-1}$) of pollutant ($p$). An individual vehicle-specific daily $VKT_{vin}$ (km d$^{-1}$) is estimated by Eq. (1). The $EF_{hot;p,v,myr,s}$ (g/km) is the hot exhaust emission factor of pollutants ($p$) for the vehicle type ($v$), vehicle manufacture year ($myr$), and average vehicle speed ($s$). The district's total emission rate is the total hot exhaust emissions from all individual vehicles within the same district.

$$E_{hot; p,vin,myr} = DF_{p,v,myr} \times VKT_{vin} \times EF_{hot; p,v,myr,s} \qquad (3)$$

The deterioration factor ($DF$) in Eq. (3) is an optional function in the CARS. The deterioration process is caused by vehicle aging and can lead to the increase of vehicle emissions. The vehicle DF is varied by vehicle type ($v$), pollutant ($p$), and vehicle manufacture year ($myr$). The CARS model computes vehicle ages based on the vehicle manufacture year and model simulation year. According to NIER's guidance on calculating deterioration factors, there is no deterioration in a new vehicle during their first five years. After five years, the deterioration factors can range from 5% to 10% depending on the type of vehicle and pollutants. Deterioration processes can cause up to an 100% increase of emissions in fifteen-year-old vehicles. Currently, the $DF$ is an empirical coefficient that varies by vehicle age (Lee et al., 2011a).

The hot exhaust emission factor, $EF_{hot;p,v,s}$ (g/km) is a function of vehicle speed ($s$) with other empirical coefficients: $a, b, c, d, f, k$. The emission factor formula and those coefficients were developed by NIER's CAPSS (Lee et al., 2011a). These coefficients are varied by pollutants ($p$), vehicle type ($v$), vehicle manufacture year ($myr$), and vehicle speed ($s$). The vehicle speed affects the combustion efficiency of an ICE and impacts the emission rates and its composition from the tailpipe.

$$EF_{hot; p,v,myr,s} = k(a \times s^b + c \times s^d + f) \qquad (4)$$

While vehicle speed plays a critical role in hot exhaust emissions from most vehicles, NOx emissions from some diesel vehicles show sensitivity to local ambient temperature and humidity due to the atmospheric moisture suppression of high combustion temperatures that lower $NO_x$ emissions at higher humidity (Choi et al., 2017; Ntziachristos and Samaras, 2000). Figure 3 shows

244    the dependency of $NO_x$ emission factors from compact diesel vehicles to vehicle speed (Fig. 3a)
245    and ambient temperature (Fig. 3b). Figure 3a shows a significant decrease of $NO_x$ emissions when
246    the speed increases between 0 and 70 km. Figure 3b demonstrates the significance of local
247    meteorology on $NO_x$ emissions from a compact diesel sedan. Based on these NIER's CAPSS
248    emission factors, the sensitivity to local ambient temperature is limited to $NO_x$ pollutant emissions
249    from diesel vehicles.

250    Due to its high sensitivity to the vehicle operating speed, it is important for the CARS to
251    simulate realistic speed patterns for accurate emissions estimates. When a single speed is assigned
252    to compute hot exhaust emissions, it won't reflect the emissions under low-speed circumstances.
253    To overcome this limitation, the CARS has adopted the 16 average speed bins concepts for a better
254    representation of vehicle speed distribution that varies by road type (i.e., local, highway,
255    expressway). We have implemented a feature for the CARS optionally to apply road-specific
256    average speed distributions (ASD) ($A_{bin,r}$) by 16 speed bins (*bin*) (from 0 to 121 km h$^{-1}$ defined in
257    Appendix E) for eight different road types (*r*) (No.101-108, shown in Appendix C) as classified
258    by CAPSS (Fig. 4a). Although ASD patterns vary by region and time, the current CARS model
259    version does not support ASD application by region and time of day due to the lack its availability
260    in South Korea.

261    We first developed the ASD (Fig. 4a) for eight different road types (No. 101-108) in South
262    Korea based on the latest road link-specific average speed and the length of link from the SK GIS
263    road network shapefiles (NIER, 2018). However, the ASD based on the SK GIS road shapefiles
264    did not capture low speed (<16 km h$^{-1}$) driving (Fig. 4a). This causes a significantly lower
265    estimation of NOx and VOC emissions compared to the CAPSS (Appendix G). We believe the
266    SK average speed distribution is missing low speed driving that can occur due to traffic congestion.
267    To address this absence of low-speed driving in the SK ASD, we incorporated data from the ASD
268    (Figure 4b) from the state of Georgia to the low speed ranges (speed bin #1 and #2 for road type 1
269    to 7). We increased the total fractions of low speed bins (the 2:1 ratio of fractions of bin #1 and
270    #2) by 2% for interstate expressways, 3% for urban expressways, 7% for all highways, and 15%
271    for all local roads. The increases in low speed bins lowered the distributions of other higher speed
272    bins homogeneously due to the renormalization of fractions by road type. Figure 4c shows the
273    renormalized hybrid-ASDs of all road types based on SK ASD and Georgia ASD. We understand
274    that the hybrid-ASD approach is not ideal for SK onroad emission inventory development, but it
275    clearly demonstrates the CARS's capability and sensitivity to the vehicle speed representation.

276    While 16 speed bins ASD application is critical to computing more realistic hot exhaust
277    emissions, there should be some restrictions on certain road types. Users can adjust the restricted
278    roads control table input file to limit the vehicle types that are only operated on a particular road
279    type. For example, motorcycles are limited to local roads (No. 104, 106, and 107), but not on
280    expressways (No. 101, 102, 103, 105, and 108) due to its traffic regulation rules. Heavy trucks are
281    only allowed on the highway (No. 101, 102, 103, 105, and 108.) by law. The details of the road

282  restriction control table format can be found on the CARS's user's guide from the CARS version
283  1 used in this paper (Baek et al., 2021).

284      The 16 speed bins ASD from Eq. (13) are added to the CARS hot exhaust emissions
285  equation (Eq. 3). The hot exhaust emissions from individual vehicles ($E_{hot;p,vin,myr}$) can be
286  calculated by considering road-specific speed bins distribution (Eq. 5). Although the vehicles may
287  be operated in different districts from their registered district, this is our best method to estimate
288  the vehicle speed for hot exhaust emissions.

289  $$E_{hot;\,p,vin,myr} = DF_{p,v,myr} \times \sum_{bin}(VKT_{vin} \times EF_{hot;\,p,v,myr,s} \times A_{bin,r}) \qquad (5)$$

290  **2.2.2  Cold Start Emissions**

291      The cold start emissions occur when a cold engine vehicle is ignited. Lower temperatures
292  of the ICE are not optimal conditions for complete fuel combustion. This process lowers the
293  combustion efficiency (CE) and increases the emissions of hydrocarbon and CO pollutants from
294  the tailpipe exhaust (Jang et al., 2007). The CARS can estimate the cold start emissions for vehicles
295  using gasoline, diesel, or liquefied petroleum gas (LPG) fuel. Besides the vehicle and engine type,
296  road type also plays a critical role in the quantity of cold start emissions because it occurs mostly
297  in parking lots and rarely on highways.

298      The cold start emission, $E_{cold}$ (g d$^{-1}$), is derived from the hot exhaust emissions, the ratio of
299  hot to cold exhaust emissions ($EF_{cold}/EF_{hot}$ -1.0), and the percentage of the traveled distance with
300  a cold engine (Eq. 6).

301  $$E_{cold;\,p,v} = \beta_T \times E_{hot;\,p,v} \times \left(\frac{EF_{cold;\,p,v}}{EF_{hot;\,p,v}} - 1.0\right) \qquad (6)$$

302      The emission factor of cold start emissions ($EF_{cold}$) is not directly calculated from
303  measurement data like hot exhaust emissions ($E_{hot;p,v}$), but measured under different ambient
304  temperatures ($T$). The CARS model applies linear regression models developed by CAPSS to
305  estimate the increasing ratio of cold start to hot exhaust emissions ($EF_{cold}/EF_{hot}$) under different
306  temperatures ($T$) (Eq. 7). In this equation, $A$ and $B$ are the empirical coefficients that vary by the
307  pollutants ($p$) and vehicle type ($v$).

308  $$(\frac{EF_{cold;\,p,v}}{EF_{hot;\,p,v}}) = A_{p,v} + B_{p,v} \times T \qquad (7)$$

309      $\beta$ is the percentage of the distance traveled under a cold engine and also depends on the
310  ambient temperature. Cold ambient temperatures cause a longer distance traveled under a cold
311  engine due to the slower heating time. According to the CAPSS database for Seoul city (Lee et al.,
312  2011a), the empirical linear equation for $\beta$ is shown in Eq. (8). This formula represents how

313  ambient temperature affects $\beta$. For example, when the average temperature is -2°C, $\beta$ is 34.8%. In
314  summer, the monthly average temperature is 25.7°C, which causes $\beta$ to drop to 21%.

315  $$\beta = 0.647 - 0.025 \times 12.35 - (0.00974 - 0.000385 \times 12.35) \times T \qquad (8)$$

### 2.2.3  Evaporative VOC Emissions

317  Evaporative emissions are emissions from vehicle fuel that are evaporated into the
318  atmosphere. This occurs in the fueling system inside the vehicle, such as fuel-tanks, injection
319  systems, and fuel lines. Diesel vehicles, however, can be exempted due to diesel fuel's low vapor
320  pressure. The primary sources of evaporative emissions are breathing losses through tank vents
321  and fuel permeation/leakage. The CARS model adopted the EEA's emission inventory guidebook
322  (EEA, 2019) to account for diurnal emissions from the tank ($e_d$), hot and warm soak emissions by
323  fuel injection type ($S_{fi}$), and running loss emissions ($R$) (Eq. 9). Unlike CAPSS, there is a
324  conversion factor (0.075) applied to $E_{vap}$ for motorcycles to prevent an overestimation of VOC.

325  $$E_{vap;\,p,v} = \left(e_{d;\,p,v} + S_{fi;\,p,v} + R_{l;\,p,v}\right) \qquad (9)$$

326  Diurnal emissions, $e_d$ (g d$^{-1}$), during the daytime are caused by the ambient temperature
327  increase and the expansion of fuel vapors inside the fuel tank. Most of the current fuel tank systems
328  have emission control systems to limit this kind of evaporative VOC emissions. The $e_d$ can be
329  calculated with the empirical Eq. (10), which was developed by CAPSS. $T_l$ is the monthly average
330  of the daily lowest temperatures and $T_h$ is the monthly average of the daily highest temperatures.
331  The empirical coefficient $\alpha$ is 0.2, which represents how 80% of emissions are eliminated by the
332  vehicle emission control system.

333  $$e_d = \alpha \times 9.1 exp \left[0.3286 + 0.0574 \times (T_l) + 0.0614 \times (T_h - T_l - 11.7)\right] \qquad (10)$$

334  Soak emissions ($S_{fi}$) occur when a hot ICE is turned off; the remaining heat from the ICE
335  can increase the fuel temperature in the system which causes the increase of evaporative VOC
336  emissions. This carburetor float bowls are the major source of the soak emissions. Newer vehicles
337  with fuel injection and returnless fuel systems do not emit soak emissions. Because most of the
338  current vehicles in South Korea have a new fuel system, soak emissions ($S_{fi}$) in the CARS model
339  are set to 0.

340  The running loss emissions ($R_l$) are from vapors generated in the fuel tank when a vehicle
341  is in operation (Eq. 11). In some older vehicles, the carburetor and engine operation can increase
342  the temperature in the fuel tank and carburetor, which can cause a significant increase in
343  evaporative VOC emissions. VOC emissions from running loss can be greatly increased during
344  warmer weather. However, newer vehicles with fuel injection and returnless fuel systems are not

345 affected by the ambient temperature. Because most vehicles in South Korea do not use carburetor
346 technology, we expect running loss emissions to have the least impact (Lee et al., 2011b).

347
$$R_l = \alpha \times L_{r,v} \times [(1 - \beta) \times R_h + \beta \times R_w] \qquad (11)$$

348 The empirical coefficient α is 0.1 here, which represents that 90% of the running loss is
349 avoided by the newer fuel system. *L* is the distance traveled (km) by road and is the same one used
350 in hot exhaust emission calculations. $\beta$ is the same parameter from Eq. (8). The $R_h$ and $R_w$ are the
351 average emission factors from running loss under hot and warm/cold conditions, respectively.

## 2.3 Road Link-Level Emissions Calculations

353 In general, district-level automobile emissions calculations are driven by district-level
354 averaged vehicle activity and operating data, which do not reflect realistic spatial patterns of
355 onroad automobile emissions. The CARS model introduces road link-specific traffic data by
356 default to develop spatially enhanced road link-specific emissions that are more representative of
357 the emissions. This high-resolution traffic data is a GIS shapefile that is composed of many
358 connected segments, which are called "road links." All road links hold information such as
359 start/end location coordinates, AADT, road link length, averaged vehicle speed, and road type (No.
360 101-108).

361 The CARS model applies link-level AADT ($AADT_{d,r,l}$, d$^{-1}$) and road length ($L_{d,r,l}$) to
362 compute the road link-specific VKT ($VKT_{d,r,l}$, km d$^{-1}$) in Eq. (12). The road links are identified by
363 district (*d*), road type (*r*), and link (*l*) labels. The road VKT is a parameter that reflects the traffic
364 activity of each road link and it is different from individual daily vehicle activity data ($VKT_{v,age}$)
365 in Eq. (1).

366
$$VKT_{d,r,l} = AADT_{d,r,l} \times L_{d,r,l} \qquad (12)$$

367 Road link-specific VKT ($VKT_{d,r,l}$) is used to redistribute the district total emissions ($E_{onroad}$)
368 from Eq. 2 into road link-level emissions. The following three weight factors are computed: the
369 district weight factors, $\omega_d$ (Eq. 13), the road type weight factors, $\omega_{d,r}$ (Eq. 14), and the road-link
370 weight factors, $\omega_{d,l}$ (Eq. 15). The weight district factors ($\omega_d$) are the renormalization of each
371 district's total VKT over state-level total VKT (*N* is the number of districts). The main reason we
372 performed the renormalization over state-level total VKT is to reflect daily traffic patterns from
373 multiple districts under the assumption that most vehicles travel within the same state. The road
374 type weight factors by district ($\omega_{r,d}$) are used to compute road-specific emissions, while road-
375 specific averaged speed distributions (ASD; $A_{s,r}$) from Eq. (5) are applied to capture vehicle
376 operating speeds by road type. The road link weight factors ($\omega_{d,l}$) are then applied to redistribute
377 the district emissions into road link-level emissions.

378

$$\omega_d = \frac{\sum_r \sum_l VKT_{d,r,l}}{\frac{1}{N} \sum_d \sum_r \sum_l VKT_{d,r,l}} \qquad (13)$$

379

$$\omega_{d,r} = \frac{\sum_l VKT_{d,r,l}}{\sum_r \sum_l VKT_{d,r,l}} \qquad (14)$$

380

$$\omega_{d,l} = \frac{VKT_{d,r,l}}{\sum_r \sum_l VKT_{d,r,l}} \qquad (15)$$

381

## 3 CARS Configuration

382

383    The CARS model is an open-source program based on Python (Guido van Rossum, 2009)
384    that allows the users to efficiently apply open-source modules to develop programs. Users can
385    easily install Python development tools and load customized packages and modules to set up the
386    CARS development environment. All CARS modules are developed using Python v3.6. Other than
387    the GIS road shapefiles, all input files are based in the ASCII CSV format, which can be easily
388    handled by both spreadsheet programs and programming languages, making it more accessible for
389    users of all skillsets. The CARS can not only estimate district-level and spatially enhanced road
390    link-level emissions, but can also generate hourly chemically speciated gridded emissions for
391    CTMs. In addition, the CARS also generates various summary reports, graphics, and
392    georeferenced plots for quality assurance.

393    The required Python modules for the CARS are: "*geopandas*," "*shapely.geometry*", and
394    "*csv*" modules to read the shapefiles and table data files. The "*NumPy*" and "*pandas*" modules
395    are used to operate the memory arrays and scientific calculations, while the "*pyproj*" module deals
396    with converting the projection coordinate systems. "*matplotlib*" is for generating any type of
397    figures/plots. Furthermore, the CARS model can also read and write Climate and Forecast (CF)-
398    compliant NetCDF-formatted files using "*NetCDF4*".

399    The first process in the CARS is "*Loading_function_path*"; it allows users to define and
400    check the input file paths. Once all input files are checked, there are six process modules in CARS
401    to process inputs, compute emissions, and generate various output files, including QA reports.
402    Figure 5 is the schematic of the CARS that consists of six process modules with various functions.
403    The six process modules are (1) "**Process activity data**", (2) "**Process emission factors**", (3)
404    "**Process shapefile**, (4) "**Calculate district emissions**", (5) "**Grid4AQM**", and (6) "**Plot figures**".
405    The main purpose of modularizing the CARS is to meet the needs of various communities, such
406    as policymakers, stakeholders, and air quality modelers. While modules (1) through (4) are
407    required to develop the district-level and road link-level emissions inventories, module (5)
408    "**Grid4AQM**" is optional depending on if users want to develop chemically-speciated gridded
409    hourly emissions for CTMs. Also, the modularity of the CARS allows users to bypass certain

410    modules if it has been previously processed without any changes. For example, if there is no
411    change in traffic activity, emission factors table, or GIS shapefiles, users do not need to run these
412    modules and can simply read the data frame outputs and then run "**Grid4AQM**" for the modeling
413    dates and domain. The "**Grid4AQM**" module will not only improve the computational time for
414    CTMs but also eliminate the need for a 3rd party emissions modeling system like SMOKE (Baek
415    and Seppanen, 2021).

416    The rectangle boxes in Fig. 5 represent the data array and the boxes with rounded edges are
417    the functions in the CARS. Details on the CARS code, input table format, and functions setup
418    information can be found on the CARS GitHub website (Pedruzzi *et al*., 2020).

419    The "**Process activity data**" module first reads the vehicle activity data, such as an
420    individual vehicle's daily total VKT based on its registered district. The "**Process emission factors**"
421    module reads and stores the emission factors table that holds all pollutant emission factors to
422    estimate the emissions for all vehicles. Meteorology-sensitive emission factors are only limited to
423    $NO_x$ pollutants. District boundary GIS shapefiles and road network shapefiles are processed
424    through "**Process shape file**" to generate the VKT-based redistribution weighting factors from Eq.
425    (13), (14) and (15) for the "**Calculate district emissions**" module to compute district-level and
426    road link-level emission rates (metric tons per year, t $yr^{-1}$).

427    The redistributed emission rates (t $yr^{-1}$) from the "**Calculate district emissions**" module
428    present annual total emission rates until district-level VKTs from the "**Process activity data**"
429    module are added. Then, the "**Grid4AQM**" module can generate CTM-ready chemically speciated
430    emissions. The "***Read_chemical***" function from the "**Grid4AQM**" module is designed to process
431    the chemical speciation profile that can convert the inventory pollutants such as CO, $NO_x$, $SO_2$,
432    $PM_{10}$, $PM_{2.5}$, VOC, and $NH_3$, into the chemically lumped model species that CTM requires for
433    chemical mechanisms, such as SAPRC (L. and Heo, 2012) and Carbon Bond version 6 (CB6)
434    (Yarwood and Jung, 2010). The "***Read_temporal***" function processes the complete set of monthly,
435    weekly, and hourly temporal allocation profiles that can convert annual total emissions to hourly
436    emissions. "***Read_griddesc***" defines the CTM-ready modeling domain and computes the gridding
437    fractions for all road link-level emissions by overlaying the modeling domain over the GIS
438    shapefiles. Once annual total emissions are chemically speciated, spatially gridded, and temporally
439    allocated into hourly emissions, the "***Gridded_emis***" function will combine emission source-level
440    conversion fractions from each function (***Read_chemical***, ***Read_temporal***, and ***Read_griddesc***) to
441    generate the CTM-ready chemically speciated, gridded hourly emissions in the NetCDF binary
442    format. The "**Plot Figures**" module is designed for generating various summary reports and
443    graphics to assist users in understanding the estimated automobile emissions inventory computed
444    by the CARS. The following section will describe the detailed processes of the "**Grid4AQM**"
445    module, which includes chemical, spatial, and temporal allocations.

446         The influence of temperature on emission processes are considered in the CARS model.
447 There are three temperature parameters in current CARS model such as "temp_max" for maximum
448 temperature, "temp_mean" for mean temperature, and "temp_min" for minimum temperature.
449 These temperature parameters will be applied to over the entire modeling domain during the
450 simulation period. Current CARS model version does not support to process gridded meteorology
451 data from the 3$^{rd}$ party meteorology models like Meteorology-Chemistry Interface Processor
452 (MCIP) from U.S. EPA., and Weather Research Forecasting (WRF) model from National Center
453 for Atmospheric Research (NCAR) yet. However, CARS can easily adopt various temporally
454 resolved temperature values by adjusting the CARS simulation period (i.e., day, week, month,
455 season, or annual).

## 3.1    Chemical Speciation

457         To support CTMs applications, the CARS needs to be able to convert inventory pollutants
458 into chemical lumped model species based on the choice of CTM chemical mechanisms. $NO_x$
459 includes nitric oxide (NO), nitrogen dioxide ($NO_2$), and nitrous acid (HONO). VOCs can represent
460 hundreds of different organic carbon species, such as benzene, acetaldehyde, and formaldehyde.
461 These grouped inventory pollutants cannot be directly imported into the chemical mechanism
462 modules in the CTM system and require chemical speciation allocation for CTMs to process them
463 during their chemical reactions. Therefore, the "**Grid4AQM**" module performs the chemical
464 species allocation step prior to the temporal and spatial allocations to generate the gridded hourly
465 emissions. The "***Read_chemical***" function in "**Grid4AQM**" module allows users to assign these
466 emission inventory pollutants to CTM-ready surrogate chemical species (a.k.a lumped chemical
467 species) by vehicle, engine, and fuel type. For example, VOC emissions from diesel busses can be
468 converted into the following composition based on its chemical allocation profile: alkanes (68%),
469 toluene (9%), xylenes (8%), alkenes (4%), ethylene (2%), benzene (1.3%), and unreactive
470 compounds (7%) when the CB6 chemical mechanism is selected. Further details on the chemical
471 speciation profile input formats are available in the CARS user's guide.

## 3.2    Spatial Allocation

473         The "**Calculate district emissions**" module calculates both total district and road link
474 specific emissions based on road link-specific AADT data from road network GIS shapefiles. The
475 "**Calculate district emissions**" module first gets the district total vehicle emissions (Eq. 2) based
476 on the district-level VKTs, and then the normalized district total emissions by district weight factor,
477 $\omega_d$ (Eq. 13). Afterwards, the normalized district total emissions are redistributed into every road
478 link using road link-level weight factors ($\omega_{d,l}$) (Eq. 15). The district total emissions from Eq. (2)
479 and from Eq. (15) remain the same. Then the computed road link-level emissions then will be

480  converted into grid cell emissions using the modeling domain grid cell fractions computed in the
481  "*Read_griddesc*" function in the "**Grid4AQM**" module.

## 3.3    Temporal Allocation

483        Once chemical and spatial allocations are completed, the final step to support CTM
484  application is a temporal allocation that converts the annual total emissions from the "**Calculate**
485  **district emissions"** module into hourly emissions. The "*Read_temporal*" temporal allocation
486  function in the "**Grid4AQM"** module converts the annual emission rate (t $yr^{-1}$) to the hourly
487  emission rate (mol $hr^{-1}$) using monthly, weekly, and weekday/weekend diurnal temporal profiles.
488  This module processes these temporal profile inputs, which are the monthly (January - December),
489  weekly (Monday - Sunday), and weekday/weekend 24-hour profile tables (0:00-23:00 LST). The
490  users can assign these temporal profiles with a combination of vehicle, engine, fuel, and road types
491  to enhance their temporal representations in detail.

## 3.4    Chemical Transport Model Emissions

493        The main goal of the **"Grid4AQM"** module is to generate temporally, chemically, and
494  spatially enhanced CTM-ready gridded hourly emissions. First, it reads the CTM modeling domain
495  configuration and then overlays it over the road network GIS shapefile and district-boundary
496  shapefile to define the modeling domain. This overlaying process between the road network,
497  district boundary GIS shapefiles, and modeling domain allows the **"Grid4AQM"** module to
498  compute the fraction of road links that intersects with each grid cell. Figure 6 demonstrates how
499  the district boundary and road network GIS shapefiles are used to perform the spatial allocation
500  processes in CARS. Figure 6a is a native road link shapefile of Seoul with AADT, VKT, district
501  ID, and road type. Figure 6b presents an overlay of two districts' road links (purple and blue) over
502  the selected region. State total emissions will be renormalized into weighed district total emission
503  data and then redistributed into the road link. Figure 6c illustrates how the weighted road link-
504  level emissions get allocated into modeling grid cells for CTMs. The link-level VKT ($VKT_{d,r,l}$)
505  from Eq. (12) will be used to compute a total of traffic activity fractions by grid cell and then use
506  that to assign the link-level emissions from Eq. (2) into each grid cell. When a road link intersects
507  with multiple grid cells, the "**Grid4AQM"** module will weigh the emissions by the length of the
508  link that intersects with each grid cell. It should be noted that current CARS model can only
509  generate the Community Multiscale Air Quality (CAMQ)-ready gridded hourly emissions in
510  format of IOAPI (Input/Output Applications Programming Interface) based on NetCDF format.

511        Through the overlay process, the CARS model can generate various types of output data,
512  such as total district emissions, link-level emissions, and CTM-ready gridded emissions. For
513  example, the CO vehicle emissions from the Seoul metropolitan in South Korea are presented in
514  three different output formats in Fig. 7. Figure 7a shows the annual mobile $PM_{2.5}$ emissions by

515    district. The road link level annual emissions are presented in Fig. 7b. Furthermore, the CARS
516    applies the link-level emissions from Fig. 7b to generate the hourly grid cell emission data with a
517    1 km × 1 km resolution for the CTM in Fig. 7c.

518    **3.5    National Control Strategy Application**

519        One of the unique features in the CARS compared to other mobile emissions models is that
520    it can promptly develop a strategy to control automobile emissions in response to   national
521    emergency high $PM_{2.5}$ episodes. It is very common to experience high $PM_{2.5}$ episodes, especially
522    during the wintertime in South Korea due to domestic and international primary and secondary air
523    pollutants emissions. When the 72-hour forecasted $PM_{2.5}$ concentration exceeds the average 50
524    $\mu g/m^3$ (0:00-16:00 LST), the national $PM_{2.5}$ emergency control strategy is activated for ten days.
525    It applies a nationwide vehicle restriction policy within 24 hours. It enforces a limit on what kind
526    of vehicles can be operated on a certain date. The restrictions can be closures of public parks and
527    government facilities and of certain vehicles based on their fuel type and age, which is a major
528    factor of engine deterioration. This policy will limit the number of vehicles on the network roads
529    significantly, which could reduce primary $PM_{2.5}$ and precursor pollutant ($NO_x$, $NH_3$, and VOC)
530    emissions, especially from heavily populated metropolitan regions (Choi et al., 2014; Kim et al.,
531    2017a; Kim et al., 2017b; Kim et al., 2017c).
532        To understand the impacts of an even or odd vehicle number restriction policy in real-time,
533    we need to quickly develop a rapid controlled response emissions for the air quality forecast
534    modeling system based on the reduced number of vehicles on the road. The process of generating
535    the controlled mobile emission inventory can take a long time if we start fresh. Thus, we have
536    implemented this control strategy as an optional "*Control Factors*" function in the "**Calculate**
537    **district emissions**" in the module for users to quickly and easily generate the controlled mobile
538    emission inventory with consideration of the limited number of vehicles based on the vehicle,
539    engine, fuel, and vehicle manufactured year. A one hundred percent (100%) control factor means
540    that there are no emissions from those selected vehicles.

541        Because of the modularization system in the CARS, we can bypass some computationally
542    expensive data processing modules (i.e., "**Process activity data**", "**Process emission factors**",
543    and "**Process shape file**") and let the "**Calculate district emissions**" module quickly apply control
544    factors while it computes the district-level mobile emission inventory from Eq. (2).  This will allow
545    users to reduce the computational time to generate the controlled mobile emissions under a specific
546    control scenario and develop the controlled CTM-ready gridded hourly emissions using the
547    "**Grid4AQM**" module.

16

## 3.6 Computational Time

While the CARS can generate a high-quality spatiotemporal emission inventory, it is quite critical for the CARS to generate them effectively and accurately without being at the expense of computational time. This is especially important to meet the needs for an air quality forecast modeling system responding to a national emergency control strategy implementation.

In this section, we will discuss the details of the CARS computational modeling performance. While the CARS model has been highly optimized, the modularization of CARS has also improved its modeling performance with its optional module runs. The breakdown of module specific computational time estimates based on the benchmark CARS runs are listed in Table 1. The benchmark CARS case includes a total of 24,383,578 daily VKT datasets from KSTA over two different years, 84,608 emission factors for all pollutants across a combination of vehicle-age-engine-fuel types, 385,795 road links from the GIS road network shapefiles, 5,150 districts/16-states boundary GIS shapefile, and 5,494 grid cells (=82 rows and 67 columns) for CTMs. Without any computational parallelization, the total processing time of all six modules usually takes around a half hour to generate a single day CTM-ready gridded hourly emission file. However, it can be further shortened to 25-30 minutes on a higher performance computer. Because of the modular system implemented in the CARS, generating one month (31 days) long gridded hourly emissions from CTMs in 100 minutes on high-performance computers. The maximum usage of RAM can reach up to 11 GB. Table 1 shows the breakdown of computational time by each module from two different hardwares (desktop and laptop computers). The numbers in parentheses beside the **"Grid4AQM"** module is the computational time for a single day versus 31 days. While the **"Grid4AQM"** module takes an average of 4.9 minutes for a single day emissions generation, processing a consecutive 31 days saves 46% more time, decreasing it from 151.9 minutes (=4.9 minutes * 31 days) to 81.6 minutes.

## 4 Results

**CARS and CAPSS Comparison**

The CARS model calculates the 2015 onroad automobile emissions based on the latest 2015 emission factors and the 2015-2017 vehicle activity database in South Korea. The annual total emissions from CARS are compared against the ones from NIER's CAPSS in Table 2. The CARS model estimated the following annual total emissions in units of metric tons per year (t yr$^{-1}$): NO$_x$ (301,794); VOC (61,186); CO (373,864), NH$_3$ (12,453); PM$_{2.5}$ (10,108), and SO$_x$ (172.0). Compared to NIER's CAPSS, the CARS underestimated NO$_x$ (-18% decrease) and SO$_x$ (-17% decrease), and overestimated the emissions of VOC by 33%, PM$_{2.5}$ by 15%, CO by 52%, and NH$_3$ by 24%. Both NIER's CAPSS and CARS shared the same emission factor tables, which hold over

582 84,608 emission factors for all pollutants across a combination of vehicle, age, engine, and fuel
583 types.

584     The difference in results between CAPSS and CARS are caused by three following reasons.
585 First, the number of vehicles used in CARS is slightly higher (6%) than CAPSS data (1.3 out of
586 23 million), as well as other key traffic-related activity inputs (i.e., vehicle age distribution,
587 averaged speed distribution, etc). Secondly, the vehicle speed information assigned by vehicle and
588 road type play a critical role. The CAPSS calculation was based on the road-specific a signle
589 average speed value or 80% of the speed limit of the road as an input of vehicle operating speed
590 for three road types (rural, urban, and expressway) (Lee et al., 2011b). In other words, CAPSS
591 only assigns a "single-speed value" for each road type, and does not encounter the variation of
592 vehicle speed during its operation on roads into the emissions calculation. Most running exhaust
593 emissions occur during a vehicle's low-speed operation due to its incomplete combustion of fuel,
594 and it is critical to accurately represent the emissions across various speed bins in order to compute
595 the accurate emissions (Fig. 4). A detailed analysis of the impact of vehicle speed will be discussed
596 later in this chapter. Lastly, other advanced processes in the CARS, such as link-level AADT and
597 district-level vehicle data (5,150 districts in South Korea) can reflect more spatial detail and
598 variation than the CAPSS. The CAPSS only considers state-level data (17 states in South Korea)
599 and five road types (interstate expressway, urban highway, rural highway, urban local, and rural
600 local).

601     Figure 8 illustrates more details about the difference in annual emissions between CARS
602 and CAPSS by pollutants and vehicle types. Sedan vehicles show the largest increase of VOC
603 (33%), CO (41%), and $NH_3$ (23%) in the CARS relative to CAPSS because almost 56% of total
604 vehicle count (13.5 million) is composed of sedan vehicles (Appendix B). In Table 3, sedan
605 vehicles contribute 51% of total VOC and 61% of total CO annual emissions. The VOC and CO
606 emissions from sedans are largely affected by the average speed distribution process when
607 compared to other vehicle types. Similarly, the largest decreases of $NO_x$ (-16%) and $SO_x$ (-18%)
608 are from trucks because they are significant $NO_x$ (~50%) and $SO_x$ contributors (~27%) and their
609 emission factors are sensitive to vehicle speed.

610 **Onroad Emissions Analysis**

611     The CARS is a bottom-up emissions model, which utilizes local individual vehicle activity
612 data, detailed local emission factors for every vehicle and fuel type, and localized inputs such as
613 average speed distribution by road type and deterioration factor. It allows users to assess a detailed
614 breakdown of localized emission contributions. Table 3 represents the individual air pollutants
615 ($NO_x$, VOC, $PM_{2.5}$, CO, $NH_3$, and $SO_x$) emission contributions (t $yr^{-1}$), fractions (%), and impact
616 factors (IF) by the vehicle type and fuel system. The IF is defined by the normalized annual
617 emissions with vehicle counts of each category (kg $yr^{-1}$ per vehicle). The CARS also can provide

18

618   the average daily VKT per vehicle, which is the total daily VKT divided by vehicle numbers, to
619   explain the emission contributions in Appendix D.

620       Diesel-fueled vehicles contribute the most $NO_x$ emissions at over 85.3% (257,305 t $yr^{-1}$),
621   although the number of diesel vehicles only amounts to approximately 35% of the total vehicles
622   (Table 3a). While diesel trucks emitted 49.1% (148,246 t $yr^{-1}$) of total $NO_x$ with an IF value of
623   47.9 (kg $yr^{-1}$), the highest impact (IF = 340 kg $yr^{-1}$) occurred from diesel buses with only an 8.51%
624   contribution to the total NOx emissions. This is caused by the highest average daily VKT from
625   diesel buses compared to other vehicles, which is expected in a highly populated metropolitan area
626   like Seoul, South Korea. A diesel bus generally has a 3-5 times higher daily VKT (180 km $d^{-1}$)
627   than other common vehicles (gasoline sedan: 34 km $d^{-1}$, diesel truck: 57 km $d^{-1}$). The second-
628   largest vehicle type is the CNG (compressed natural gas) bus (248 kg $yr^{-1}$), which also has a high
629   VKT at an average daily of 212 km $d^{-1}$ with only a 3.1% $NO_x$ contribution.

630       For VOC emissions, over 12 million gasoline vehicles cause 52.1% (31,885 t $yr^{-1}$) of the
631   total VOC emissions, with the gasoline sedan as the highest contributor (46.5% at 14,070 t yr-1)
632   across all vehicle types (Table 3b). Diesel vehicles only contribute 23.0% (14,070 t $yr^{-1}$) of the
633   total VOC emissions. The IF values from VOC indicate that CNG buses have the highest, which
634   is 247 kg $yr^{-1}$ (19% over total VOC) with a low number of heavy CNG vehicles. The IF of the
635   CNG bus is the highest which is 320 kg $yr^{-1}$ and emits 19.5% of the total VOC. Comparing the IFs
636   of buses across fuel types, the CNG bus emits less $NO_x$ but higher VOC than a diesel vehicle. Each
637   CNG bus has about 33 times higher IF of VOC (320 kg $yr^{-1}$) than a diesel bus (9.51 kg $yr^{-1}$), and
638   CNG buses release slightly lower $NO_x$ (248 kg $yr^{-1}$) than diesel buses (340 kg $yr^{-1}$) (Table 3a and
639   3b).

640       The South Korea NIER currently does not have the PM emission factors from tire and
641   brake wear, which are the highest contributors of $PM_{2.5}$ emissions from onroad vehicles (Hugo
642   A.C. et al., 2013; Fulvio Amato et al., 2014). Once the emission factors of tire and brake wear are
643   prepared, those emissions can be computed by CARS. For that reason, diesel vehicles become the
644   major source of $PM_{2.5}$ emissions, which contributes over 98.5% (9,959 t $yr^{-1}$) of the $PM_{2.5}$
645   emissions based on the CARS 2015 emissions (Table 3c). The diesel truck, SUV, and van are three
646   major sources of total $PM_{2.5}$ at 53.6%, 21.4%, and 11.2%, respectively. Although over 52% of the
647   vehicles are gasoline vehicles, their primary $PM_{2.5}$ contribution is limited to 1.44%. The diesel
648   bus has the highest IF (2.83 kg $yr^{-1}$), which is caused by the largest average daily VKTs.

649       Similar to VOC emissions, CO is mostly emitted through the tailpipe due to incomplete
650   internal combustion of fuel and share similar emissions distributions across vehicle and fuel types
651   (Table 3d). Gasoline vehicles contribute most of the CO (220,390 t $yr^{-1}$, 59.0%), and sedan vehicles
652   are the primary source (178,121 t $yr^{-1}$, 47.6%) of this out of all gasoline vehicles. Across vehicle
653   types, buses show the highest IF of CO (81.2 kg $yr^{-1}$) due to its largest daily VKT. CO is the most
654   abundant pollutant released from vehicles (373,864 t $yr^{-1}$) across all pollutants from onroad

19

automobile sources. Although CO is much less reactive than other vehicle VOCs (Rinke and Zetzsch, 1984; Liu and Sander, 2015), CO emissions play a critical role in generating 30% of all hydroperoxyl radicals ($HO_2$) and cause ozone formation in urban areas (Pfister et al., 2019). Thus, CO is also another crucial precursor to ozone formation in urban areas.

$SO_x$ emissions are related to the sulfur content within the fuel component. Diesel has the highest sulfur content than any other fuels and consequently most $SO_x$ is contributed by diesel vehicles (93.8 t $yr^{-1}$, 54.5%) (Table 3e). Within diesel vehicles, trucks provide 26.5% of $SO_x$ (45. t $yr^{-1}$). Although the $SO_x$ from sedan vehicles are slightly higher (~3.3%) than diesel trucks, the number of diesel trucks is only 29.6% of the number of gasoline sedans. Thus, diesel trucks have a higher IF than gasoline sedans. Across vehicle types, buses have the highest IF (0.095 kg $yr^{-1}$) of $SO_x$, and diesel buses in particular have the largest IF at 0.143 kg $yr^{-1}$.

The $NH_3$ emissions table (table 3f) indicates that 98.7% of $NH_3$ is from gasoline vehicles while diesel trucks only contribute 1.13%. The IF result also shows that the gasoline sedan has the most significant impact per vehicle (1.17 kg $yr^{-1}$).

According to the vehicle activity and the CARS model results, nearly half of the total vehicles (24.3 million) are gasoline sedans (10.4 million, 42.8%), and gasoline sedan vehicles contribute the majority of VOC and CO emissions (46.5% and 47.6%), but only 7.7% of the total $NO_x$ emissions. The number of diesel vehicles is at 8.6 million (35.4%); however, they emit about 85.3% of the total $NO_x$ and 98.5% of the primary $PM_{2.5}$. These results indicate that the annual traffic-related automobile emissions are not only affected by the number of vehicles, but also by vehicle and fuel types and age of vehicles. Therefore, this study normalized the annual emissions by the number of vehicles to confirm the emission composition by individual vehicle types.

**Average Speed Impact Study**

The CARS can also optionally apply the average speed distribution (ASD) by road type to compute more realistic mobile emissions on the road network when compared to using a current single average speed value for each road type (Appendix E). Applying the ASD will generate a better representation of actual traffic patterns from each road type. To understand the impacts of ASD application, we performed sensitivity runs between using a single speed to the ASD application (Appendix F). The ASD data was described in Fig. 4, and the road-specific average single speed values were developed based on the weighted average method using the same ASD data. Appendix E and S6 describe the details of ASD as well as road-specific speed values.

Figure 9a shows the differences in total emissions between two scenarios and is organized by pollutant. The single-speed scenario largely underestimates the emissions across all pollutants compared to the ones from the ASD scenario. $NO_x$ (16%), VOC (40%), and CO (30%) were especially underestimated. The difference is caused by the lack of low-speed bins (<16 km $h^{-1}$) representation when a single average speed approach was used. Higher emissions are emitted while

20

691 vehicles are operated with low-speed bins, which decreases the combustion efficiency of ICE and
692 releases more pollutants.

693 Figure 9b shows the road-specific emissions breakdown between the ASD and single speed
694 approaches to understand the impacts of vehicle operating speeds on onroad automobile emissions.
695 In this figure, each color indicates the emissions percentage differences by road types. Other than
696 $NH_3$, the most significant discrepancies are from urban local roads, highways, and urban highways,
697 respectively. This pattern is caused by a better presentation of low-speed conditions ($<16$ km h$^{-1}$)
698 in CAR simulation (Appendix C). The lower speeds cause the incomplete combustion of ICE and
699 increase the emission rate. Also, local urban roads, highways, and urban highways have higher
700 road VKT contributions at 17%, 18%, and 12%, respectively (Appendix C) than rural ones. A
701 better presentation of low-speed operating vehicles from highly travelled roads (urban local, urban
702 highway, and highway) caused these significant differences between the ASD and single-speed
703 approaches. Although the interstate expressway has the largest VKT contribution (41%), it also
704 has the lowest fraction of low-speed bins (2%). That is why the difference between the ASD and
705 single speed scenarios on interstate expressways is less than 1%. In general, $NH_3$ emission factors
706 do not change by vehicle operating speed, so the ASD impact is quite minimal.

## 5   Conclusions

708 The CARS is a bottom-up automobile emissions model that utilizes the localized traffic-
709 related activity and emission factors input datasets to generate high quality localized emissions
710 inventories for policymakers, stakeholders, and research community as well as temporally and
711 spatially enhanced hourly gridded emissions for CTMs. First, the CARS model employs the daily
712 VKTs for all registered vehicles and the emission factors function to compute district-level total
713 daily emissions for each vehicle. To reflect realistic traffic patterns, the CARS model computes
714 and utilizes link-level VKTs (=link-length×AADT) from the road network GIS shapefiles to
715 redistribute the original district-level total emissions into spatially enhanced road link-level
716 emissions. It can also optionally implement a control strategy as well as road restriction rules to
717 improve the quality of local emission inventories and meet the needs of users.

718 The CARS model is a fully modularized and computationally optimized python-based
719 model that can effectively process a huge dataset to calculate high quality spatiotemporal county-
720 level, road link-level, and grid cell-level mobile emissions. We believe that the implementation of
721 the ASD into the CARS improves the representation of onroad automobile emissions from the
722 road network when compared to a single speed for each road type. It additionally allows the CARS
723 to have a better representation of low speed ($<16$ km h-1) vehicle emissions. We believe that CARS
724 model's versatile spatiotemporal bottom-up automobile emissions and the in-depth analysis feature
725 can assist government policymakers and stakeholders to quickly develop responsive emission

726 strategies to South Korea's national PM$_{2.5}$ emergency control strategy that enforces the nationwide
727 vehicle restriction policy within 24 hours.

## Code Availability:

729 The source code of the CARS model public release version 1.0 can be downloaded from the
730 Github release website:

731 https://doi.org/10.5281/zenodo.5033314
732
733

**Digital Object Identifier (DOI) for the CARS version 1.0:**

735 https://doi.org/10.5281/zenodo.5033314
736
737

**Installation Package for CARS version 1.0:**

739 The CARS version 1.0 installation package comes with the complete inputs and outputs datasets
740 for users to confirm their proper installation on their computers and can be downloaded from the
741 CARS version 1 used in this paper (Baek et al., 2021):
742 https://doi.org/10.5281/zenodo.5033314
743
744

**User's Guide Documentation:**

746 The CARS version user's guide documentation can be accessed through the the CARS version 1
747 used in this paper (Baek et al., 2021):
748 https://doi.org/10.5281/zenodo.5033314
749 https://github.com/bokhaeng/CARS/tree/master/docs/User_Manual
750

## Data availability:

752 All the datasets, excel, and python scripts used in this manuscript for the data analysis are
753 uploaded through GMD website along with a supplemental appendix document.
754

## Author contribution

756 Dr. B.H. Baek and Dr. Jung-Hun Woo are the lead researchers in this study. Dr. Rizzieri
757 Pedruzzi developed the source code of CARS model, Dr. Minwoo Park tested the model and
758 provided the model input data. Dr. Chi-Tsan Wang analyzed the model results and prepared the
759 manuscript. Younha Kim and Chul-Han Song also analyzed the model results and provided
760 comments.

761
762

## Competing interests

764     The authors declare that they have no conflict of interest.

## Acknowledgments

772

# References

Safety flare for burning combustible gas - has tangential inlet for non-flammable gas between housing and stack, in, Shell Oil Co (Shel-C).

Anaconda, Anaconda python: https://www.anaconda.com/products/individual, last access: May, 1st, 2020.

Appel, W., Chemel, C., Roselle, S., Francis, X., Hu, R.-M., Sokhi, R., Rao, S. T., and Galmarini, S.: Examination of the Community Multiscale Air Quality (CMAQ) model performance over the North American and European domains, Atmospheric Environment, 53, 142–155, 10.1016/j.atmosenv.2011.11.016, 2013.

Baek, B. H., Pedruzzi, Rizzieri, Wang, Chi-Tsan, Woo, Jung-Hun (2021). bokhaeng/CARS: CARS (Comprehensive Automobile Emissions Research Simulator) version 1.0 Public Release (CARSv1.0). Zenodo. https://doi.org/10.5281/zenodo.5033314

Baek, B. H., and Seppanen, C., SMOKE v4.8.1 Public Release (January 29, 2021). (Version SMOKEv481_Jan2021): http://doi.org/10.5281/zenodo.4480334.

Burnett, R., Chen, H., Szyszkowicz, M., Fann, N., Hubbell, B., Pope, C. A., Apte, J. S., Brauer, M., Cohen, A., Weichenthal, S., Coggins, J., Di, Q., Brunekreef, B., Frostad, J., Lim, S. S., Kan, H., Walker, K. D., Thurston, G. D., Hayes, R. B., Lim, C. C., Turner, M. C., Jerrett, M., Krewski, D., Gapstur, S. M., Diver, W. R., Ostro, B., Goldberg, D., Crouse, D. L., Martin, R. V., Peters, P., Pinault, L., Tjepkema, M., van Donkelaar, A., Villeneuve, P. J., Miller, A. B., Yin, P., Zhou, M., Wang, L., Janssen, N. A. H., Marra, M., Atkinson, R. W., Tsang, H., Quoc Thach, T., Cannon, J. B., Allen, R. T., Hart, J. E., Laden, F., Cesaroni, G., Forastiere, F., Weinmayr, G., Jaensch, A., Nagel, G., Concin, H., and Spadaro, J. V.: Global estimates of mortality associated with long-term exposure to outdoor fine particulate matter, Proceedings of the National Academy of Sciences, 115, 9592, 10.1073/pnas.1803222115, 2018.

Choi, D., Beardsley, M., Brzezinski, D., Koupal, J., and Warila, J.: MOVES Sensitivity Analysis: The Impacts of Temperature and Humidity on Emissions
, available at: https://www3.epa.gov/ttn/chief/conference/ei19/session6/choi.pdf  2017.

Choi, K.-C., Lee, J.-J., Bae, C. H., Kim, C.-H., Kim, S., Chang, L.-S., Ban, S.-J., Lee, S.-J., Kim, J., and Woo, J.-H.: Assessment of transboundary ozone contribution toward South Korea using

803  multiple source–receptor modeling techniques, Atmospheric Environment, 92, 118-129,
804  https://doi.org/10.1016/j.atmosenv.2014.03.055, 2014.


805  Cohen, A. J., Brauer, M., Burnett, R., Anderson, H. R., Frostad, J., Estep, K., Balakrishnan, K.,
806  Brunekreef, B., Dandona, L., Dandona, R., Feigin, V., Freedman, G., Hubbell, B., Jobling, A.,
807  Kan, H., Knibbs, L., Liu, Y., Martin, R., Morawska, L., Pope, C. A., III, Shin, H., Straif, K.,
808  Shaddick, G., Thomas, M., van Dingenen, R., van Donkelaar, A., Vos, T., Murray, C. J. L., and
809  Forouzanfar, M. H.: Estimates and 25-year trends of the global burden of disease attributable to
810  ambient air pollution: an analysis of data from the Global Burden of Diseases Study 2015, The
811  Lancet, 389, 1907-1918, 10.1016/S0140-6736(17)30505-6, 2017.
812


813  Dennis, R., Fox, T., Fuentes, M., Gilliland, A., Hanna, S., Hogrefe, C., Irwin, J., Rao, S. T.,
814  Scheffe, R., Schere, K., Steyn, D., and Venkatram, A.: A FRAMEWORK FOR EVALUATING
815  REGIONAL-SCALE NUMERICAL PHOTOCHEMICAL MODELING SYSTEMS, Environ
816  Fluid Mech (Dordr), 10, 471-489, 10.1007/s10652-009-9163-2, 2010.


817  EEA: EMEP/EEO air pollutant emission inventory guidebook 2016, 2019.


818  Enthought, Enthought Canapy Python:  https://assets.enthought.com/downloads/edm/, last
819  access: May, 1st, 2020.


820  Fallahshorshani, M., André, M., Bonhomme, C., and Seigneur, C.: Coupling Traffic, Pollutant
821  Emission, Air and Water Quality Models: Technical Review and Perspectives, Procedia - Social
822  and Behavioral Sciences, 48, 1794-1804, https://doi.org/10.1016/j.sbspro.2012.06.1154, 2012.


823  Fulvio Amato, Flemming R. Cassee, Hugo A.C. Denier van der Gon, Robert Gehrig, Mats
824  Gustafsson, Wolfgang Hafner, Roy M. Harrison, Magdalena Jozwicka, Frank J. Kelly,
825  TeresaMoreno, Andre S.H. Prevot, Martijn Schaap, Jordi Sunyer, Xavier Querol, Urban air
826  quality:The challenge of traffic non-exhaust emissions, Journal of Hazardous Materials, 275, 31-
827  36, https://doi.org/10.1016/j.jhazmat.2014.04.053, 2014.
828


829  Guevara, M., Tena, C., Porquet, M., Jorba, O., and Pérez García-Pando, C.: HERMESv3, a
830  stand-alone multi-scale atmospheric emission modelling framework – Part 1: global and regional
831  module, Geosci. Model Dev., 12, 1885-1907, 10.5194/gmd-12-1885-2019, 2019.


832  Hogrefe, C., Rao, S. T., Kasibhatla, P., Hao, W., Sistla, G., Mathur, R., and McHenry, J.:
833  Evaluating the performance of regional-scale photochemical modeling systems: Part II—ozone

834 predictions, Atmospheric Environment, 35, 4175-4188, https://doi.org/10.1016/S1352-
835 2310(01)00183-2, 2001a.


836 Hogrefe, C., Rao, S. T., Kasibhatla, P., Kallos, G., Tremback, C. J., Hao, W., Olerud, D., Xiu,
837 A., McHenry, J., and Alapaty, K.: Evaluating the performance of regional-scale photochemical
838 modeling systems: Part I—meteorological predictions, Atmospheric Environment, 35, 4159-
839 4174, https://doi.org/10.1016/S1352-2310(01)00182-0, 2001b.


840 Hugo A.C. Denier van der Gon, Miriam E. Gerlofs-Nijland, Robert Gehrig, Mats Gustafsson,
841 Nicole Janssen, Roy M. Harrison, Jan Hulskotte, Christer Johansson, Magdalena Jozwicka,
842 Menno Keuken, Klaas Krijgsheld, Leonidas Ntziachristos, Michael Riediker & Flemming R.
843 Cassee: The Policy Relevance of Wear Emissions from Road Transport, Now and in the
844 Future—An International Workshop Report and Consensus Statement, Journal of the Air &
845 Waste Management Association, 63:2, 136-149, DOI: 10.1080/10962247.2012.741055, 2013
846


847 Ibarra-Espinosa, S., Ynoue, R., amp, apos, Sullivan, S., Pebesma, E., Andrade, M. d. F., and
848 Osses, M.: VEIN v0.2.2: an R package for bottom–up vehicular emissions inventories, Geosci.
849 Model Dev., 11, 2209-2229, 10.5194/gmd-11-2209-2018, 2018a.


850 Ibarra-Espinosa, S., Ynoue, R., O'Sullivan, S., Pebesma, E., Andrade, M. D. F., and Osses, M.:
851 VEIN v0.2.2: an R package for bottom–up vehicular emissions inventories, Geosci. Model Dev.,
852 11, 2209-2229, 10.5194/gmd-11-2209-2018, 2018b.


853 IEMA, Inventário de Emissões Atmosféricas do Transporte Rodoviário de Passageiros no
854 Município de São Paulo.: http://emissoes.energiaeambiente.org.br, last access: May,1st, 2017.


855 Jang, Y. K., Cho, K. L., Kim, K., Kim, H. J., and Kim, J.: Development of methodology for
856 esimation of air pollutants emissions and future emissions from on-road mobile sources.,
857 National Institute of Environmental Research, Incheon, Korea., available at:  2007.


858 Kaewunruen, S., Sussman, J. M., and Matsumoto, A.: Grand Challenges in Transportation and
859 Transit Systems, Frontiers in Built Environment, 2, 10.3389/fbuil.2016.00004, 2016.


860 Kim, B.-U., Bae, C., Kim, H. C., Kim, E., and Kim, S.: Spatially and chemically resolved source
861 apportionment analysis: Case study of high particulate matter event, Atmospheric Environment,
862 162, 55-70, https://doi.org/10.1016/j.atmosenv.2017.05.006, 2017a.

863    Kim, H. C., Kim, E., Bae, C., Cho, J. H., Kim, B. U., and Kim, S.: Regional contributions to
864    particulate matter concentration in the Seoul metropolitan area, South Korea: seasonal variation
865    and sensitivity to meteorology and emissions inventory, Atmos. Chem. Phys., 17, 10315-10332,
866    10.5194/acp-17-10315-2017, 2017b.

867    Kim, H. C., Kim, S., Kim, B.-U., Jin, C.-S., Hong, S., Park, R., Son, S.-W., Bae, C., Bae, M.,
868    Song, C.-K., and Stein, A.: Recent increase of surface particulate matter concentrations in the
869    Seoul Metropolitan Area, Korea, Scientific Reports, 7, 4710, 10.1038/s41598-017-05092-8,
870    2017c.

871    L., W. P., and Heo, G.: Development of revised SAPRC aromatics mechanism, available at:
872    https://www.engr.ucr.edu/~carter/SAPRC/saprc11.pdf  2012.

873    Lee, D., Lee, Y.-M., Jang, K.-W., Yoo, C., Kang, K.-H., Lee, J.-H., Jung, S.-W., Park, J.-M.,
874    Lee, S.-B., Han, J.-S., Hong, J.-H., and Lee, S.-J.: Korean National Emissions Inventory System
875    and 2007 Air Pollutant Emissions, Asian Journal of Atmospheric Environment, 5-4, 278-291,
876    2011a.

877    Lee, D.-G., Lee, Y.-M., Jang, K.-W., Yoo, C., Kang, K.-H., Lee, J.-H., Jung, S.-W., Park, J.-M.,
878    Lee, S.-B., Han, J.-S., Hong, J.-H., and Lee, S.-J.: Korean National Emissions Inventory System
879    and 2007 Air Pollutant Emissions, Asian Journal of Atmospheric Environment, 5,
880    10.5572/ajae.2011.5.4.278, 2011b.

881    Lejri, D., Can, A., Schiper, N., and Leclercq, L.: Accounting for traffic speed dynamics when
882    calculating COPERT and PHEM pollutant emissions at the urban scale, Transportation Research
883    Part D: Transport and Environment, 63, 588-603, https://doi.org/10.1016/j.trd.2018.06.023,
884    2018.

885    Li, F., Zhuang, J., Cheng, X., Li, M., Wang, J., and Yan, Z.: Investigation and Prediction of
886    Heavy-Duty Diesel Passenger Bus Emissions in Hainan Using a COPERT Model, Atmosphere,
887    10, 106, 10.3390/atmos10030106, 2019.

888    Li, Q., Qiao, F., and yu, L.: Vehicle Emission Implications of Drivers Smart Advisory System
889    for Traffic Operations in Work Zones, Journal of the Air & Waste Management Association, 11,
890    10.1080/10962247.2016.1140095, 2016.

891    Liu, H., Guensler, R., Lu, H., Xu, Y., Xu, X., and Rodgers, M.: MOVES-Matrix for High-
892    Performance On-Road Energy and Running Emission Rate Modeling Applications, Journal of
893    the Air & Waste Management Association, 69, 10.1080/10962247.2019.1640806, 2019.

894 Liu, Y., and Sander, S. P.: Rate Constant for the OH + CO Reaction at Low Temperatures, The
895 Journal of Physical Chemistry A, 119, 10060-10066, 10.1021/acs.jpca.5b07220, 2015.

896 Luo, H., Astitha, M., Hogrefe, C., Mathur, R., and Rao, S. T.: A new method for assessing the
897 efficacy of emission control strategies, Atmospheric Environment, 199, 233-243,
898 https://doi.org/10.1016/j.atmosenv.2018.11.010, 2019.

899 Lv, W., Hu, Y., Li, E., Liu, H., Pan, H., Ji, S., Hayat, T., Alsaedi, A., and Ahmad, B.: Evaluation
900 of vehicle emission in Yunnan province from 2003 to 2015, J. Clean Prod., 207, 814-825,
901 https://doi.org/10.1016/j.jclepro.2018.09.227, 2019.

902 Moussiopoulos, N., Vlachokostas, C., Tsilingiridis, G., Douros, I., Hourdakis, E., Naneris, C.,
903 and Sidiropoulos, C.: Air quality status in Greater Thessaloniki Area and the emission reductions
904 needed for attaining the EU air quality legislation, Sci. Total Environ., 407, 1268-1285,
905 https://doi.org/10.1016/j.scitotenv.2008.10.034, 2009.

906 Nagpure, A. S., Gurjar, B. R., Kumar, V., and Kumar, P.: Estimation of exhaust and non-exhaust
907 gaseous, particulate matter and air toxics emissions from on-road vehicles in Delhi, Atmospheric
908 Environment, 127, 118-124, 10.1016/j.atmosenv.2015.12.026, 2016.

909 NIER: Study on Air Pollutant Emission Estimation Method in Transportation section(II) 11-
910 1480523-003573-01, National Archives of Korea, available at:
911 https://www.archives.go.kr/next/manager/publishmentSubscriptionDetail.do?prt_seq=114054&p
912 age=1554&prt_arc_title=&prt_pub_kikwan=&prt_no 2018.

913 Ntziachristos, L., and Samaras, Z.: Speed-dependent representative emission factors for catalyst
914 passenger cars and influencing parameters, Atmospheric Environment, 34, 4611-4619,
915 https://doi.org/10.1016/S1352-2310(00)00180-1, 2000.

916 Ntziachristos, L., Gkatzoflias, D., Kouridis, C., and Samaras, Z.: COPERT: A European road
917 transport emission inventory model, 491-504 pp., 2009.

918 Pedruzzi, R., Baek, B. H., and Wang, C.-T., CARS: https://github.com/CMASCenter/CARS,
919 last access: MAy, 1st, 2020.

920 Perugu, H., Ramirez, L., and DaMassa, J.: Incorporating temperature effects in California's on-
921 road emission gridding process for air quality model inputs, Environ Pollut, 239, 1-12,
922 10.1016/j.envpol.2018.03.094, 2018.

923 Perugu, H.: Emission modelling of light-duty vehicles in India using the revamped VSP-based
924 MOVES model: The case study of Hyderabad, Transportation Research Part D: Transport and
925 Environment, 68, 150-163, https://doi.org/10.1016/j.trd.2018.01.031, 2019.


926 Pfister, G., Wang, C.-t., Barth, M., Flocke, F., Vizuete, W., and Walters, S.: Chemical
927 Characteristics and Ozone Production in the Northern Colorado Front Range, JGR, 2019.


928 Pinto, J. A., Kumar, P., Alonso, M. F., Andreão, W. L., Pedruzzi, R., dos Santos, F. S., Moreira,
929 D. M., and Albuquerque, T. T. d. A.: Traffic data in air quality modeling: A review of key
930 variables, improvements in results, open problems and challenges in current research,
931 Atmospheric Pollution Research, 11, 454-468, https://doi.org/10.1016/j.apr.2019.11.018, 2020.


932 Rao, S. T., Galmarini, S., and Puckett, K.: Air Quality Model Evaluation International Initiative
933 (AQMEII): Advancing the State of the Science in Regional Photochemical Modeling and Its
934 Applications, Bulletin of the American Meteorological Society, 92, 23-30,
935 10.1175/2010BAMS3069.1, 2011.


936 Rodriguez-Rey et al. (2021): Rodriguez-Rey, D., Guevara, M., Linares, MP., Casanovas, J.,
937 Salmerón, J., Soret, A.,Jorba, O., Tena, C., Pérez García-Pando, C.: A coupled macroscopic
938 traffic and pollutant emission modelling system for Barcelona, Transportation Research Part D,
939 92, https://doi.org/10.1016/j.trd.2021.102725, 2021.


940 Rinke, M., and Zetzsch, C.: Rate Constants for the Reactions of OH Radicals with Aromatics:
941 Benzene, Phenol, Aniline, and 1,2,4-Trichlorobenzene, Berichte der Bunsengesellschaft für
942 physikalische Chemie, 88, 55-62, 10.1002/bbpc.19840880114, 1984.


943 Russell, A., and Dennis, R.: NARSTO critical review of photochemical models and modeling,
944 Atmospheric Environment, 34, 2283-2324, https://doi.org/10.1016/S1352-2310(99)00468-9,
945 2000.


946 Ryu, J. H., Han, J. S., Lim, C. S., Eom, M. D., Hwang, J. W., Yu, S. H., Lee, T. W., Yu, Y. S.,
947 and Kim, G. H.: The Study on the Estimation of Air Pollutants from Auto- mobiles (I) -
948 Emission Factor of Air Pollutants from Middle and Full sized Buses., in, Transportation
949 Pollution Research Center, National Institute of Environmental Research, Incheon, Korea., 2003.


950 Ryu, J. H., Lim, C. S., Yu, Y. S., Han, J. S., Kim, S. M., Hwang, J. W., Eom, M. D., Kim, G. Y.,
951 Jeon, M. S., Kim, Y. H., Lee, J. T., and Lim, Y. S.: The Study on the Esti- mation of Air
952 Pollutants from Automobiles (II) - Emis- sion Factor of Air Pollutants from Diesel Truck., in,

953 Trans- portation Pollution Research Center, National Institute of Environmental Research,
954 Incheon, Korea., 2004.

955 Ryu, J. H., Yu, Y. S., Lim, C. S., Kim, S. M., Kim, J. C., Gwon, S. I., Jeong, S. W., and Kim, D.
956 W.: The Study on the Estimation of Air Pollutants from Automobiles (III) - Emission Factor of
957 Air Pollutants from Small sized Light-duty Vehicles., in, Transportation Pollution Research
958 Center, National Institute of Environmental Research, Korea., 2005.

959 Sallis, P., Bull, F., Burdett, P., Frank, P., Griffiths, P., Giles-Corti, P., and Stevenson, M.: Use of
960 science to guide city planning policy and practice: How to achieve healthy and sustainable future
961 cities, The Lancet, 388, 10.1016/S0140-6736(16)30068-X, 2016.

962 Smit, R., Kingston, P., Neale, D. W., Brown, M. K., Verran, B., and Nolan, T.: Monitoring on-
963 road air quality and measuring vehicle emissions with remote sensing in an urban area,
964 Atmospheric Environment, 218, 116978, https://doi.org/10.1016/j.atmosenv.2019.116978, 2019.

965 Sun, W., Duan, N., Yao, R., Huang, J., and Hu, F.: Intelligent in-vehicle air quality
966 management : a smart mobility application dealing with air pollution in the traffic, 2016.

967 Tominaga, Y., and Stathopoulos, T.: Ten questions concerning modeling of near-field pollutant
968 dispersion in the built environment, Build. Environ., 105, 390-402,
969 https://doi.org/10.1016/j.buildenv.2016.06.027, 2016.

970 USEPA: Population and Activity of Onroad Vehicles in MOVES3, in, edited by: USEPA, 2020.

971 WHO, Ambient air pollution- a major threat to health and climate:
972 https://www.who.int/airpollution/ambient/en/, last 2019.

973 Xu, X., Liu, H., Anderson, J. M., Xu, Y., Hunter, M. P., Rodgers, M. O., and Guensler, R. L.:
974 Estimating Project-Level Vehicle Emissions with Vissim and MOVES-Matrix, Transportation
975 Research Record, 2570, 107-117, 10.3141/2570-12, 2016.

976 Yarwood, G., and Jung, J.: UPDATES TO THE CARBON BOND MECHANISM FOR
977 VERSION 6 (CB6), 2010.
978

979     **Tables**

980     **Table 1**. Computational processing time by CARS module based on the modeling setup: Total
981     number of activity data = 24,383,578; Emission Factors = 84,608; GIS road links=385,795;
982     districts/states=5,150/16; 9km×9km grid cells=5,494 (82 columns× 67 columns).

| No | Module | Desktop i7 (minutes) | Laptop i9 (minutes) | Averaged Time (minutes) |
|---|---|---|---|---|
| 1 | **Process activity data** | 1.8 | 1.5 | 1.7 |
| 2 | **process emission factors** | 1.1 | 0.8 | 1.0 |
| 3 | **Process shape file** | 9.9 | 7.3 | 8.6 |
| 4 | **Calculate district emissions** | 6.4 | 5.7 | 6.1 |
| 5 | **Grid4AQM** [31days] | 4.8 [75.9] | 5.0 [87.2] | 4.9 [81.6] |
| 6 | **Plot figures** | 6.2 | 5.4 | 5.8 |
| | Total [31days] | 30.2 [101.3] | 25.7 [107.9] | 28.1[104.8] |

983
984
985

986 **Table 2**. The total emissions comparison between CARS and CAPSS for the 2015 emission.

| Emission Inventory | Pollutants (t yr$^{-1}$) | | | | | |
|---|---|---|---|---|---|---|
| | NO$_x$ | VOC | PM2.5 | CO | SO$_x$ | NH$_3$ |
| CARS 2015 | **301,794** | **61,186** | **10,108** | **373,864** | **172** | **12,453** |
| CAPSS 2015 | 369,585 | 46,145 | 8,817 | 245,516 | 209 | 10,079 |

987

988

989 **Table 3**. The summary tables of emissions (t yr⁻¹), contributions (%), and impact factor (IF, kg yr⁻
990 ¹) per vehicle for criteria air pollutants (CAPs) by vehicle and fuel types: (a) for NOₓ; (b) VOC;
991 (c) for PM₂.₅; (d) for CO; (e) for SOₓ; and (f) for NH₃.

992
993 (a) NOx

| Vehicle | Gasoline | | Diesel | | LPG | | CNG | | Hybrid | | Total | |
|---|---|---|---|---|---|---|---|---|---|---|---|---|
| | Emission | IF | Emission | IF | Emission | IF | Emission | IF | Emission | IF | Emission | IF |
| Sedan | 20,219 (6.70%) | 1.94 | 14,783 (4.90%) | 12.8 | 8,159 (2.77%) | 4.49 | 12 (0.00%) | 1.26 | 65 (0.02%) | 0.39 | 43,239 (14.3%) | 3.19 |
| Truck | 23 (0.01%) | 5.54 | **148,246 (49.1%)** | 47.9 | 920 (0.31%) | 4.55 | 88 (0.03%) | 66.4 | - | - | **149,277 (49.5%)** | 45.2 |
| Bus | 0 (0.00%) | 0.97 | 25,677 (8.51%) | **340** | - | - | 9,260 (3.07%) | 248 | 0 (0.00%) | 1.77 | 34,938 (11.6%) | **333** |
| SUV | 159 (0.05%) | 1.19 | 39,565 (13.1%) | 11.4 | 175 (0.06%) | 8.54 | 0 (0.00%) | 1.60 | 1 (0.00%) | 0.42 | 39,900 (13.2%) | 11.0 |
| Van | 14 (0.00%) | 4.78 | 16,659 (5.52%) | 22.6 | 1,337 (0.44%) | 6.80 | 0 (0.00%) | 1.25 | 0 (0.00) | 0.37 | 18,012 (6.00%) | 19.2 |
| Taxi | - | - | - | - | 1,217 (0.40%) | 2.11 | - | - | - | - | 1,217 (0.40%) | 2.11 |
| Special | 1 (0.00%) | 20.1 | 12,347 (4.10%) | 152 | 0 (0.00%) | 0.52 | - | - | - | - | 12,375 (4.10%) | 151 |
| Motorcycle | 2,836 (0.94%) | 1.31 | - | - | - | - | - | - | - | - | 2,836 (0.94%) | 1.32 |
| Total | 23,253 (7.70%) | 1.83 | **257,305 (85.3%)** | 29.9 | 11,809 (3.91%) | 4.20 | 9,361 (3.10%) | **36.7** | 66 (0.02%) | 0.39 | 301,794 (100%) | 13.3 |

994
995 (b) VOC

| Vehicle | Gasoline | | Diesel | | LPG | | CNG | | Hybrid | | Total | |
|---|---|---|---|---|---|---|---|---|---|---|---|---|
| | Emission | IF | Emission | IF | Emission | IF | Emission | IF | Emission | IF | Emission | IF |
| Sedan | 28,434 (46.5%) | 2.73 | 629 (1.03%) | 0.55 | 2,107 (3.44%) | 1.16 | 3 (0.01%) | 0.33 | 77 (0.13%) | 0.47 | **31,250 (51.1%)** | 2.30 |
| Truck | 23 (0.04%) | 5.44 | 8,194 (13.4%) | 2.65 | 286 (0.47%) | 1.41 | 102 (0.17%) | 77.2 | - | - | 8,605 (14.1%) | 2.61 |
| Bus | 0 (0.00%) | 1.65 | 717 (1.17%) | 9.51 | - | - | 11,942 (19.5%) | 320 | 0 (0.00%) | 0 | 12,659 (20.7%) | **112** |
| SUV | 246 (0.40%) | 1.84 | 2,441 (3.99%) | 0.71 | 46 (0.08%) | 2.25 | 0 (0.00%) | 0.75 | 1 (0.00%) | 0.55 | 2,733 (4.47%) | 0.76 |
| Van | 21 (0.03%) | 7.04 | 1,185 (1.94%) | 1.61 | 393 (0.64%) | 2.00 | 0 (0.00%) | 0.45 | 0 (0.00%) | 0 | 1,599 (2.61%) | 1.71 |
| Taxi | - | - | - | - | 273 (0.45%) | 0.47 | - | - | - | - | 273 (0.45%) | 0.47 |
| Special | 1 (0.00%) | 25.8 | 904 (1.48%) | 11.1 | 0 (0.00%) | 0.23 | - | - | - | - | 905 (1.48%) | 11.0 |
| Motorcycle | 3,160 (5.16%) | 1.46 | - | - | - | - | - | - | - | - | 3,160 (5.16%) | 1.46 |
| Total | **31,885 (52.1%)** | 2.50 | 14,070 (23.0%) | 1.64 | 3,106 (5.08%) | 1.10 | 12,047 (19.7%) | **247** | 78 (0.13%) | 0.47 | 61,186 (100%) | 2.51 |

996
997 (c) PM2.5

| Vehicle | Gasoline | | Diesel | | LPG | | CNG | | Hybrid | | Total | |
|---|---|---|---|---|---|---|---|---|---|---|---|---|
| | Emission | IF | Emission | IF | Emission | IF | Emission | IF | Emission | IF | Emission | IF |
| Sedan | 144 (1.42%) | 0.01 | 809 (8.00%) | 0.70 | 0 | 0 | 0 | 0 | 3 (0.03%) | 0.02 | 956 (9.46%) | 0.07 |
| Truck | 0 (0.01%) | 0 | **5,415 (53.6%)** | 1.75 | 0 | 0 | 0 | 0 | - | - | **5,415 (53.6%)** | 1.64 |
| Bus | 0 | 0 | 214 (2.11%) | **2.83** | - | - | 0 | 0 | 0 (0.01%) | 0.09 | 214 (2.11%) | 1.89 |
| SUV | 2 (0.02%) | 0.02 | 2,165 (21.4%) | 0.63 | 0 | 0 | 0 | 0 | 0 | 0.02 | 2,167 (21.4%) | 0.60 |
| Van | 0 | 0 | 1,127 (11.2%) | 1.53 | 0 | 0 | 0 | 0 | 0 | 0.02 | 1,127 (11.2%) | 1.20 |
| Taxi | - | - | - | - | 0 | 0 | - | - | - | - | 0 | 0 |
| Special | 0 | 0 | 230 (2.28%) | 2.82 | 0 | 0 | - | - | - | - | 230 (2.28%) | **2.81** |
| Motorcycle | 0 | 0 | - | - | - | - | - | - | - | - | 0 | 0 |
| Total | 146 (1.44%) | 0.01 | **9,959 (98.5%)** | **1.16** | 0 | 0 | 0 | 0 | 3 (0.03%) | 0.02 | 10,108 (100%) | 0.41 |

998
999

33

1000
1001    (d) CO

| Vehicle | Gasoline | | Diesel | | LPG | | CNG | | Hybrid | | Total | |
|---|---|---|---|---|---|---|---|---|---|---|---|---|
| | Emission | IF | Emission | IF | Emission | IF | Emission | IF | Emission | IF | Emission | IF |
| Sedan | 178,121 (47.6%) | 17.1 | 3,436 (0.92%) | 2.98 | 42,886 (11.5%) | 23.6 | 29 (0.01%) | 2.91 | 177 (0.05%) | 1.07 | **224,649 (60.1%)** | 16.6 |
| Truck | 254 (0.07%) | 61.1 | 47,065 (12.6%) | 15.2 | 9,088 (2.43%) | 44.9 | 68 (0.02%) | 51.4 | - | - | 56,475 (15.1%) | 17.1 |
| Bus | 0 (0.00%) | 19.3 | 7,633 (2.05%) | **101** | - | - | 1542 (0.41%) | 41.3 | 1 (0.00%) | 4.64 | 9,176 (2.45%) | **81.2** |
| SUV | 2,616 (0.70%) | 19.6 | 13,401 (3.58%) | 3.87 | 791 (0.21%) | 38.6 | 0 (0.00%) | 4.09 | 2 (0.00%) | 1.15 | 16,808 (4.50%) | 4.65 |
| Van | 131 (0.04%) | 43.4 | 6,611 (1.77%) | 8.97 | 8,032 (2.15%) | 40.9 | 2 (0.00%) | 6.53 | 0 (0.00%) | 1.00 | 14,777 (3.95%) | 15.8 |
| Taxi | - | - | - | - | 8,481 (2.27%) | 14.7 | - | - | - | - | 8,481 (2.27%) | 14.7 |
| Special | 13 (0.00%) | 269 | 4,224 (1.13%) | 51.7 | 1 (0.00%) | 3.69 | - | - | - | - | 4,239 (1.13%) | 51.7 |
| Motorcycle | 39,256 (10.5%) | 18.2 | - | | - | - | - | - | - | - | 39,256 (10.5%) | 18.2 |
| Total | **220,390 (59.0%)** | 17.3 | 82,372 (22.0%) | 9.57 | 69,281 (18.5%) | **24.6** | 1641 (0.44%) | 33.6 | 180 (0.05%) | 1.07 | 373,864 (100%) | 15.4 |

1002
1003    (e) SO$_x$

| Vehicle | Gasoline | | Diesel | | LPG | | CNG | | Hybrid | | Total | |
|---|---|---|---|---|---|---|---|---|---|---|---|---|
| | Emission | IF | Emission | IF | Emission | IF | Emission | IF | Emission | IF | Emission | IF |
| Sedan | 51.3 (29.8%) | 0.005 | 6.5 (3.79%) | 0.006 | 8.28 (4.81%) | 0.005 | 0 | 0 | 1.14 (0.67%) | 0.007 | **67.2 (39.1%)** | 0.005 |
| Truck | 0.03 (0.02%) | 0.008 | 45.5 (26.5%) | 0.015 | 0.97 (0.57%) | 0.005 | 0 | 0 | - | - | 46.5 (27.1%) | 0.014 |
| Bus | 0 (0.00%) | 0.003 | 10.8 (6.26%) | **0.143** | - | - | 0 | 0 | 0.01 (0.01%) | 0.047 | 10.8 (6.26%) | **0.095** |
| SUV | 0 (0.00%) | 0.000 | 18.2 (10.6%) | 0.005 | 0.00 (0.00%) | 0.000 | 0 | 0 | 0.01 (0.01%) | 0.007 | 18.2 (10.6%) | 0.005 |
| Van | 0.02 (0.01%) | 0.006 | 5.5 (3.20%) | 0.007 | 0.77 (0.45%) | 0.004 | 0 | 0 | 0 (0.00%) | 0.010 | 6.30 (3.66%) | 0.007 |
| Taxi | - | - | - | - | 7.71 (4.49%) | 0.013 | - | - | - | - | 7.71 (4.48%) | 0.013 |
| Special | 0 (0.00%) | 0.003 | 7.3 (4.27%) | 0.090 | 0.00 (0.00%) | 0.005 | - | - | - | - | 7.34 (4.27%) | 0.090 |
| Motorcycle | 7.94 (4.62%) | 0.004 | - | | - | - | - | - | - | - | 7.94 (4.62%) | 0.004 |
| Total | 59.3 (34.5%) | 0.006 | **93.8 (54.5%)** | **0.011** | 17.7 (10.3%) | 0.006 | 0 | 0 | 1.17 (0.68%) | 0.007 | 172 (100%) | 0.007 |

1004
1005
1006    (e) NH$_3$

| Vehicle | Gasoline | | Diesel | | LPG | | CNG | | Hybrid | | Total | |
|---|---|---|---|---|---|---|---|---|---|---|---|---|
| | Emission | IF | Emission | IF | Emission | IF | Emission | IF | Emission | IF | Emission | IF |
| Sedan | 12,225 (98.3%) | **1.17** | 20 (0.16%) | 0.02 | 0 | 0.00 | 0 | 0 | 19 (0.15%) | 0.11 | **12,284 (98.6%)** | **0.91** |
| Truck | 0 (0.00%) | 0.03 | 82 (0.66%) | 0.03 | 0 | 0.00 | 0 | 0 | - | - | 82 (0.66%) | 0.02 |
| Bus | 0 (0.00%) | 0.09 | 15 (0.12%) | 0.19 | - | - | 0 | 0 | 0 (0.00%) | 0.51 | 15 (0.12%) | 0.13 |
| SUV | 0 (0.00%) | 0.00 | 0 (0.00%) | 0.00 | 0 | 0.00 | 0 | 0 | 0 (0.00%) | 0.16 | 0 (0.00%) | 0.00 |
| Van | 0 (0.00%) | 0.02 | 14 (0.11%) | 0.02 | 0 | 0.00 | 0 | 0 | 0 (0.00%) | 0.09 | 14 (0.11%) | 0.01 |
| Taxi | - | - | - | - | 0 | 0.00 | - | - | - | - | 0 (0.00%) | 0.00 |
| Special | 0 (0.00%) | 0.01 | 10 (0.08%) | 0.12 | 0 | 0.00 | - | - | - | - | 10 (0.08%) | 0.12 |
| Motorcycle | 49 (0.39%) | 0.02 | - | | - | - | - | - | - | - | 49 (0.39%) | 0.02 |
| Total | **12,293 (98.7%)** | **0.97** | 141 (1.13%) | 0.02 | 0 | 0.00 | 0 | 0 | 19 (0.16%) | 0.12 | 12,453 (100%) | 0.51 |

1007
1008
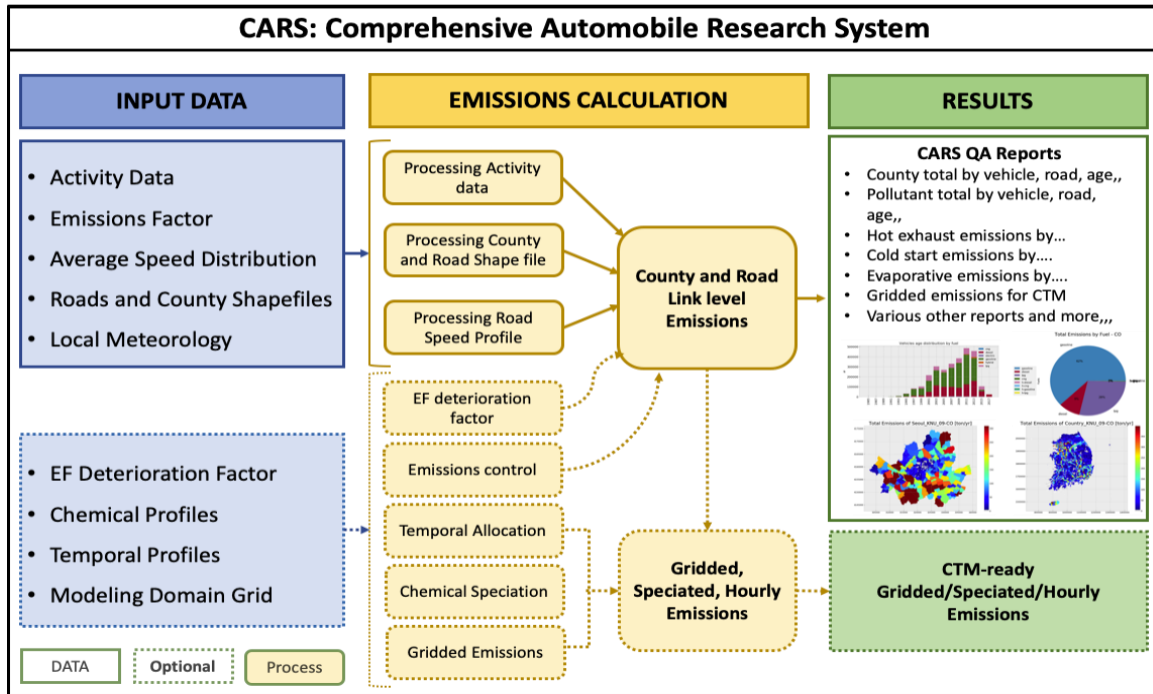
**Figures**

1011    **Figure 1**. CARS schematic methodology to estimate mobile emissions.

1012
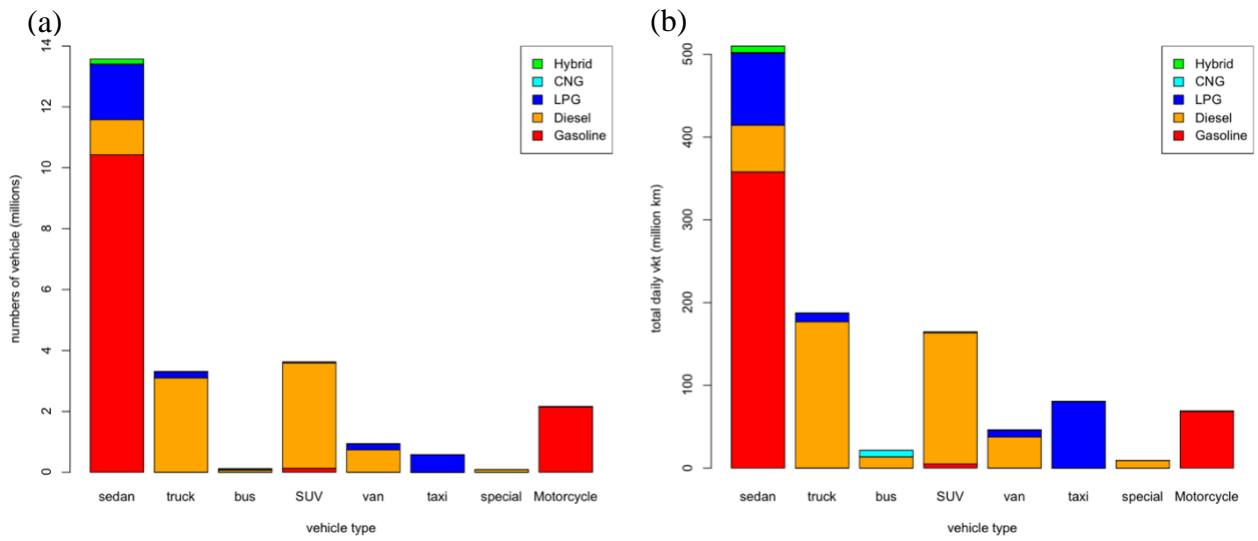
1013

1014 **Figure 2. (a)** The number of vehicles by vehicle and fuel types and **(b)** the total daily VKT by
1015 vehicle and fuel types in South Korea.

1016
1017
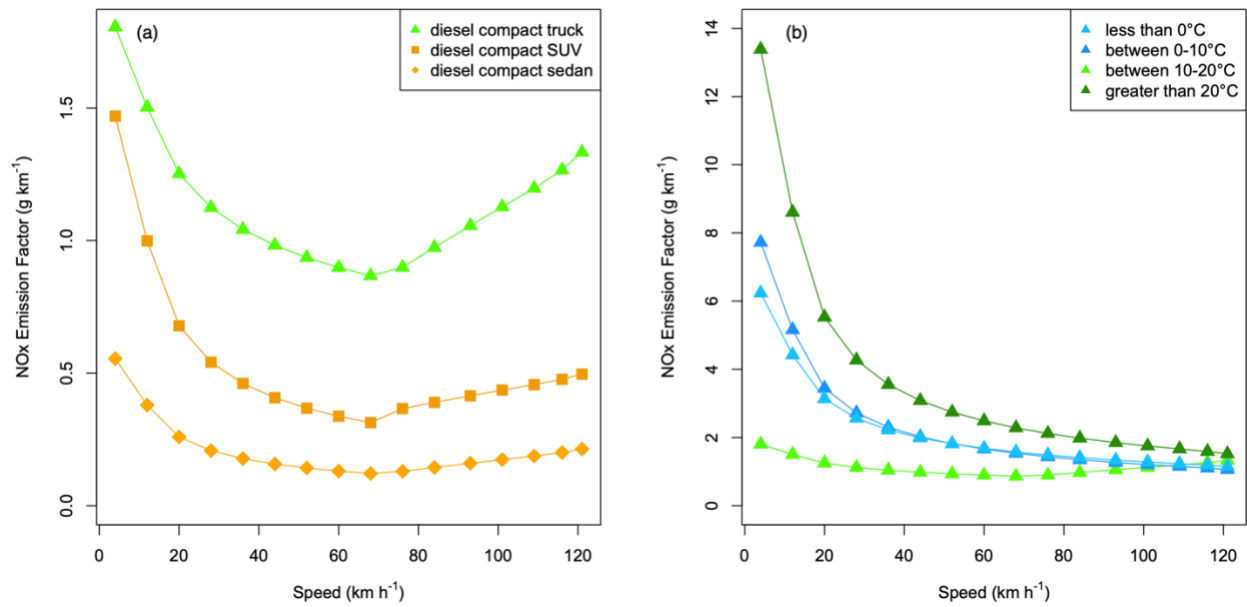
1018

**Figure 3**. Variation of NOx emission factors from diesel compact engines by vehicle speed and ambient temperatures: **(a)** $NO_x$ emission factors function to vehicle speed; **(b)** $NO_x$ emission factors of diesel compact truck function to vehicle speed and ambient temperature.

1022

(a)

(b)

1023 (c)

1024

**Figure 4**. (a) The South Korea speed distribution by road types. (b) The Georgia state speed distribution by road types. (c) The average speed distribution (ASD) by road types used in this study for South Korea.
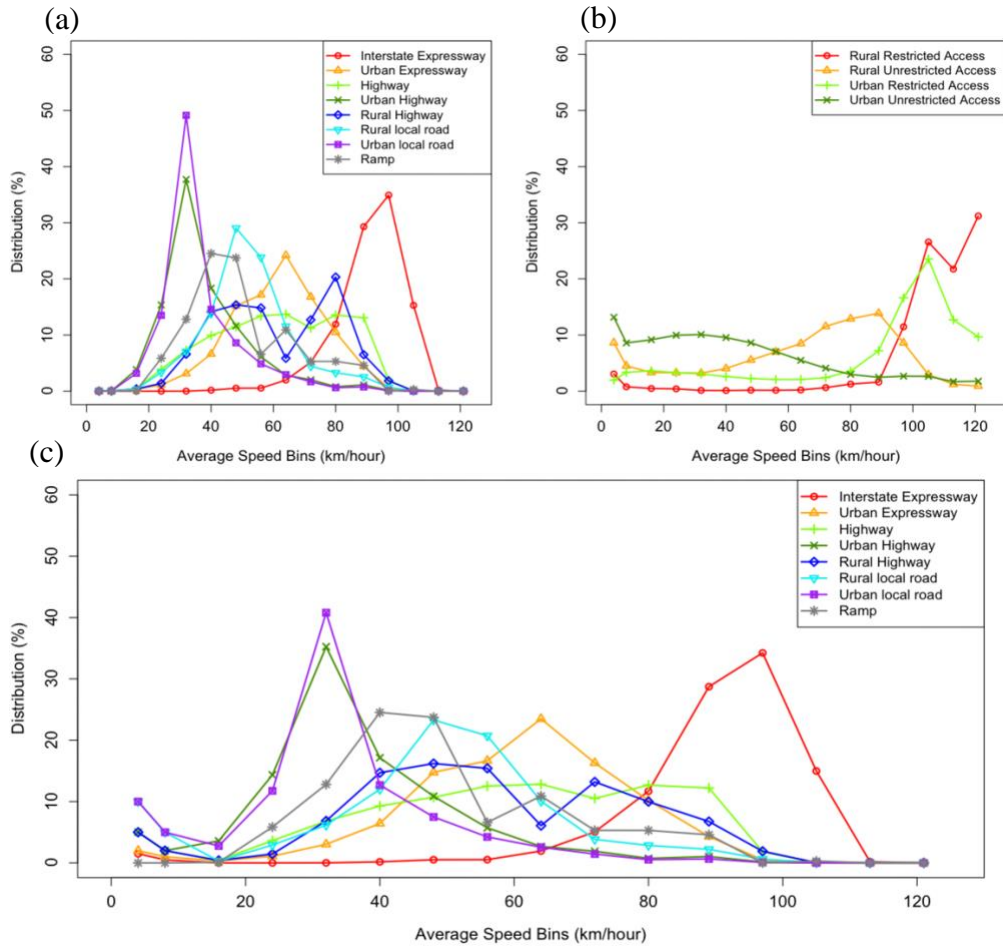
1025
1026
1027
1028
1029
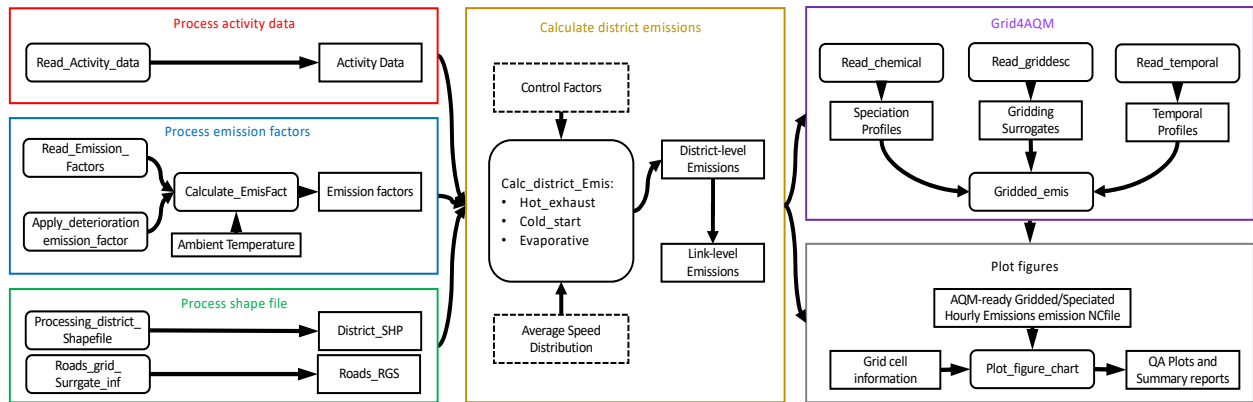
**Figure 5**. The schematic of modules and their functions in the CARS.
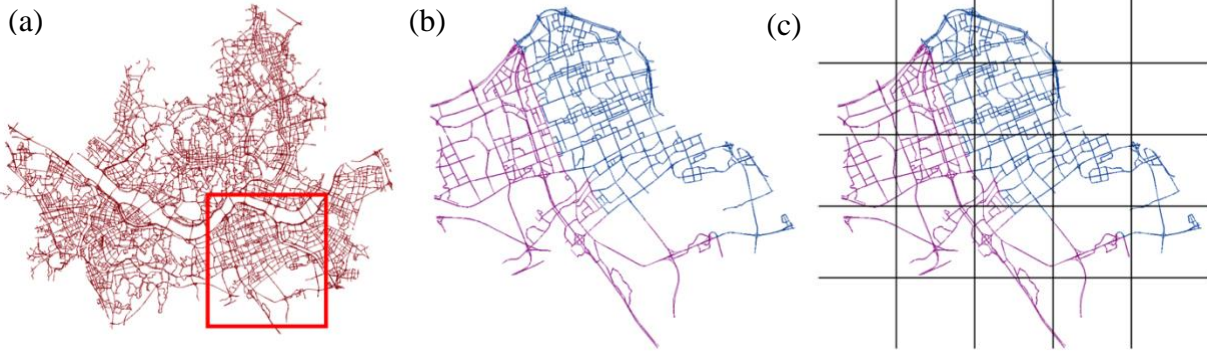
1033
1034 **Figure 6 (a)** the road network GIS shapefile of Seoul, South Korea; **(b)** two districts with different
1035 colors (purple and blue); **(c)** the modeling grid cells over road segments.
1036
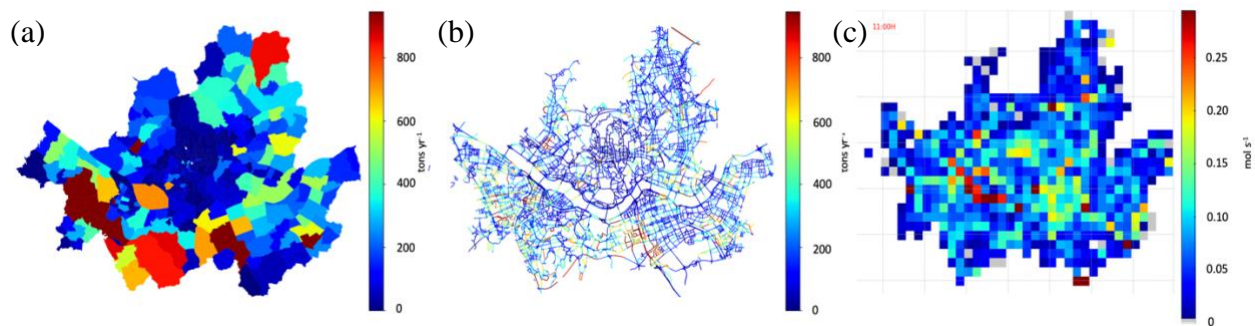
**Figure 7**. Three different formats of CO emissions from CARS, (A) District-level total emissions (t yr$^{-1}$) (B) Link-level total emissions (t yr$^{-1}$), (C) CTM-ready gridded hourly total emissions (moles s$^{-1}$).
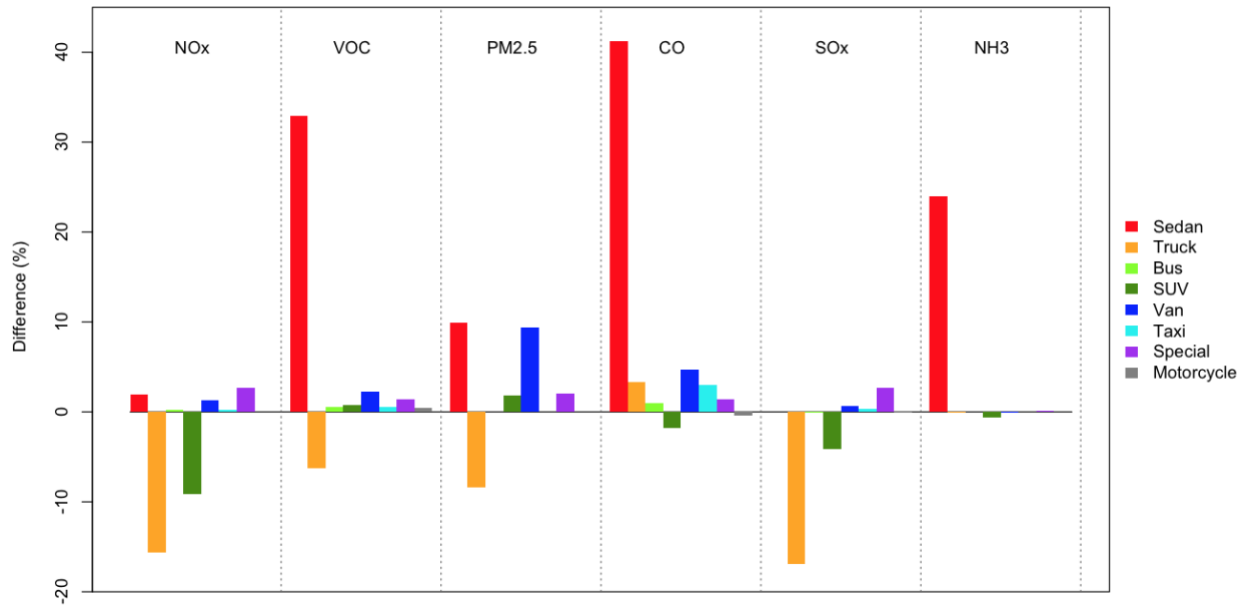
1042
**Figure 8**. Comparison between CARS 2015 and CAPSS 2015 onroad mobile emissions
inventories by vehicle types. The standard line is CAPSS 2015 data.
1045

1046
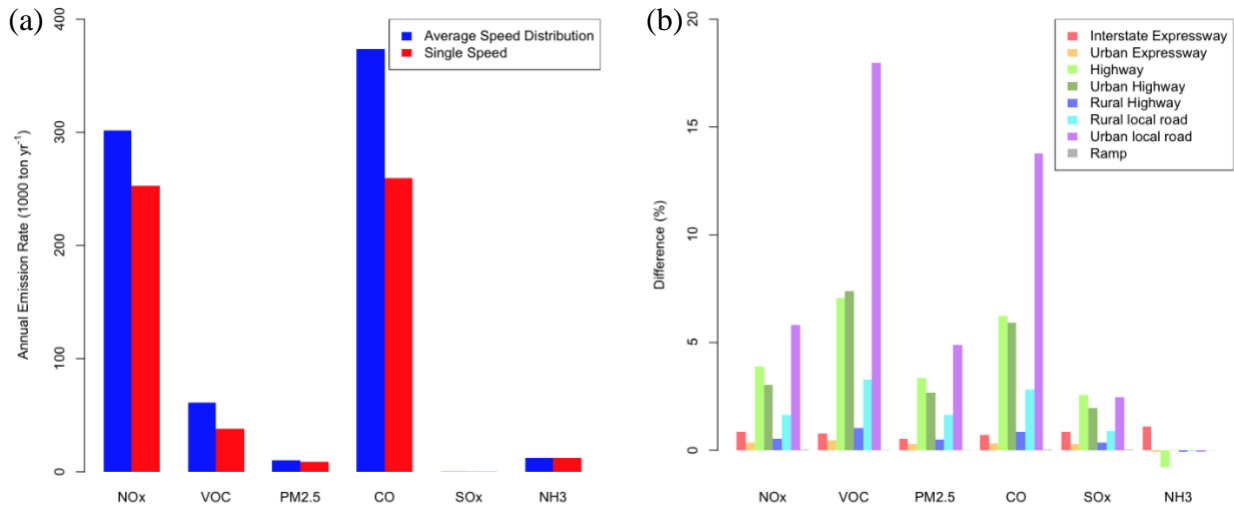


1047

**Figure 9**. The impacts of emissions between the ASD and single-speed approach: (a) the total emission differences by pollutant; (b) The road-specific difference (%) by pollutant.

1050

# Appendices


**Appendix A**: The vehicle types classified by fuel type, vehicle body type, and engine size. The emission factors of the diesel vehicle with the star (*) are depended on the ambient temperature (*T*).

| Vehicle Types | Fuel Types | | | | | | | |
|---|---|---|---|---|---|---|---|---|
| | Gasoline | Diesel | LPG | CNG | HYBRID_G | HYBRID_D | HYBRID_L | HYBRID_C |
| Sedan | Supercompact | Supercompact* | Supercompact | - | - | - | - | - |
| | Compact | compact* | compact | compact | compact | compact | compact | - |
| | Fullsize | Fullsize* | Fullsize | Fullsize | Fullsize | Fullsize | Fullsize | - |
| | Midsize | Midsize* | Midsize | Midsize | Midsize | Midsize | Midsize | - |
| Truck | Supercompact | Supercompact | Supercompact | - | - | - | - | - |
| | Compact | Compact* | Compact | Compact | - | - | - | - |
| | Fullsize | Concrete | - | Fullsize | - | - | - | - |
| | Midsize | Fullsize | Midsize | Midsize | - | - | - | - |
| | - | Midsize | - | - | - | - | - | - |
| | - | Dump | - | - | - | - | - | - |
| | - | Special | Special | Special | - | - | - | - |
| Bus | Urban | Urban | Urban | Urban | - | Urban | - | - |
| | - | Rural | - | Rural | - | Rural | - | Rural |
| SUV | Compact | Compact* | Compact | - | - | - | - | - |
| | Midsize | Midsize* | Midsize | Midsize | Midsize | - | - | - |
| Van | supercompact | supercompact | supercompact | - | - | - | - | - |
| | Compact | Compact | Compact | Compact | - | - | - | - |
| | - | - | Fullsize | Fullsize | Fullsize | Fullsize | Fullsize | Fullsize |
| | Midsize | Midsize | Midsize | Midsize | Midsize | Midsize | Midsize | Midsize |
| Taxi | - | - | Compact | - | - | - | - | - |
| | - | - | Fullsize | - | - | - | - | - |
| | - | - | Midsize | - | - | - | - | - |
| Special | - | Tow | - | - | - | - | - | - |
| | Wrecking | Wrecking | Wrecking | Wrecking | - | - | - | - |
| | Others | Others | Others | - | - | - | - | - |
| Motorcycle | Compact | - | - | - | - | - | - | - |
| | Midsize | - | - | - | - | - | - | - |
| | Fullsize | - | - | - | - | - | - | - |

- no existence
* ambient temperature-dependent diesel vehicle
LPG: Liquefied Petroleum Gas
CNG: Connecticut Natural Gas
Hybrid_G: hybrid vehicle with gasoline
Hybrid_D: hybrid vehicle with diesel
Hybrid_L: hybrid vehicle with LPG
Hybrid_C: hybrid vehicle with CNG

**Appendix B**, The summary of activity data (number of vehicles and daily total VKTs) in South
1068  Korea by vehicle type with engine size.

| Vehicle Types | Engine sizes | Fuel Types | | | | | | | | | |
|---|---|---|---|---|---|---|---|---|---|---|---|
| | | Gasoline | | Diesel | | LPG | | CNG | | Hybrid | |
| | | Numbers | Daily VKT | Numbers | Daily VKT | Numbers | Daily VKT | Numbers | Daily VKT | Numbers | Daily VKT |
| Sedan | Supercompact | 1,792,471 | 50,197,345 | 46 | 1,761 | 83,226 | 4,000,067 | 6 | 237 | - | - |
| | Compact | 1,372,317 | 39,543,668 | 51,324 | 2,570,086 | 8,040 | 257,060 | 276 | 12,115 | 3,802 | 137,360 |
| | Fullsize | 2,403,327 | 100,632,702 | 428,831 | 20,928,552 | 292,850 | 15,910,588 | 5,296 | 323,852 | 21,533 | 1,086,509 |
| | Midsize | 4,858,533 | 167,454,032 | 672,960 | 33,126,318 | 1,431,970 | 66,640,378 | 4,310 | 625,717 | 140,527 | 6,717,856 |
| Truck | Supercompact | 850 | 9,595 | 816 | 354 | 111,051 | 6,550,476 | - | - | - | - |
| | Compact | 3,185 | 143,510 | 2,655,089 | 133,480,216 | 87,650 | 3,567,109 | 42 | 2,694 | - | - |
| | Fullsize | 3 | 422 | 180,991 | 25,774,819 | - | - | 72 | 4,676 | - | - |
| | Midsize | 98 | 7,430 | 258,509 | 17,477,685 | 1,434 | 47,870 | 14 | 483 | - | - |
| | Dump | - | - | - | - | - | - | - | - | - | - |
| | Special | 20 | 970 | - | - | 2,292 | 99,124 | 1,194 | 60,886 | - | - |
| Bus | Urban | 1 | 126 | 40,448 | 7,282,593 | 1 | 652 | 6,543 | 1,466,854 | 2 | 282 |
| | Rural | - | - | 34,997 | 6,334,278 | - | - | 30,792 | 6,460,001 | 216 | 50,873 |
| SUV | Compact | 42,348 | 1,395,153 | 2,341,397 | 105,962,626 | 6,946 | 275,728 | 13 | 551 | - | - |
| | Midsize | 91,002 | 3,520,552 | 1,120,128 | 5,277,861 | 13,567 | 595,426 | 15 | 706 | 1,719 | 88,683 |
| Van | supercompact | 88 | 1,645 | - | - | 44,947 | 2,058,014 | - | - | - | - |
| | Compact | 2,937 | 87,507 | 685,317 | 34,781,937 | 151,654 | 6,135,138 | 7 | 255 | - | - |
| | Fullsize | - | - | 19,452 | 1,318,221 | 1 | 14 | 97 | 7,598 | 3 | 136 |
| | Midsize | 2 | 1,303,795 | 31,790 | 1,433,407 | 15 | 416 | 160 | 15,216 | 2 | 85 |
| | Special | - | | - | | - | | - | | - | |
| Taxi | Compact | - | - | - | - | 8,380 | 576,378 | - | - | - | - |
| | Fullsize | - | - | - | - | 92,861 | 10,827,756 | - | - | - | - |
| | Midsize | - | - | - | - | 474,455 | 69,087,721 | - | - | - | - |
| Special | Tow | - | - | 40,807 | 7,447,773 | - | - | - | - | - | - |
| | Wrecking | 2 | 138 | 12,568 | 813,746 | 128 | 6,607 | 3 | 94 | - | - |
| | Others | 47 | 553 | 28,275 | 989,988 | 180 | 9,966 | - | - | - | - |
| Motorcycle | Compact | 184,822 | 3,507,948 | - | - | - | - | - | - | - | - |
| | Fullsize | 65,964 | 3,493,728 | - | - | - | - | - | - | - | - |
| | Midsize | 1,910,988 | 61,676,824 | - | - | - | - | - | - | - | - |

1069  - no existence
1070  LPG: Liquefied Petroleum Gas
1071  CNG: Connecticut Natural Gas
1072  Hybrid: all hybrid vehicles, electric power mixed with fossil fuel (gasoline, diesel, LPG, or CNG)

1073
1074
1075

1076

1077 **Appendix C**, Eight road types with assigned average vehicle operating speed and VKT fractions.

| Road types | Description | Average Speed (km h$^{-1}$) | Road VKT fraction |
|---|---|---|---|
| 101 | Interstate Expressway | 90 | 41% |
| 102 | Urban Expressway | 60 | 5% |
| 103 | Highway | 58 | 18% |
| 104 | Urban Highway | 36 | 12% |
| 105 | Rural Highway | 55 | 3% |
| 106 | Rural Local Road | 45 | 4% |
| 107 | Urban Local Road | 32 | 17% |
| 108 | Ramp | 50 | 0.4% |

1078
1079

1080 **Appendix D,** The daily average VKT (km d$^{-1}$) per vehicle by vehicle and fuel types.

| Vehicle types | Fuel Types | | | | | |
|---|---|---|---|---|---|---|
| | Gasoline | Diesel | LPG | CNG | Hybrid | Average |
| Sedan | 34 | 49 | 48 | 97 | 48 | 38 |
| Truck | 39 | 57 | 51 | 52 | - | 57 |
| Bus | 126 | 180 | - | 212 | 237 | 191 |
| SUV | 37 | 46 | 42 | 45 | 52 | 46 |
| VAN | 29 | 51 | 42 | 87 | 44 | 49 |
| Taxi | - | - | 140 | - | - | 140 |
| Special | 14 | 113 | 54 | 31 | - | 113 |
| Motorcycle | 32 | - | - | - | - | 32 |

1081

1082

**Appendix E**, Average speed distribution (ASD) for each road type: The table columns are different road types, and the table rows are average speed of each speed bin.

| Speed bins | Speed (km/h) | Road Types 101 | 102 | 103 | 104 | 105 | 106 | 107 | 108 |
|---|---|---|---|---|---|---|---|---|---|
| 1 | speed < 4 | 1.50% | 2.00% | 5.00% | 5.00% | 5.00% | 10.00% | 10.00% | 0.00% |
| 2 | 4 ≤ speed < 8 | 0.50% | 1.00% | 2.00% | 2.00% | 2.00% | 5.00% | 5.00% | 0.00% |
| 3 | 8 ≤ speed < 16 | 0.00% | 0.33% | 0.40% | 3.59% | 0.41% | 0.30% | 2.76% | 0.11% |
| 4 | 16 ≤ speed < 24 | 0.00% | 1.09% | 3.64% | 14.35% | 1.45% | 2.91% | 11.75% | 5.85% |
| 5 | 24 ≤ speed < 32 | 0.01% | 3.04% | 6.82% | 35.25% | 6.85% | 6.15% | 40.80% | 12.80% |
| 6 | 32 ≤ speed < 40 | 0.17% | 6.43% | 9.28% | 17.14% | 14.70% | 12.00% | 12.69% | 24.53% |
| 7 | 40 ≤ speed < 48 | 0.52% | 14.76% | 10.70% | 10.86% | 16.20% | 23.30% | 7.49% | 23.74% |
| 8 | 48 ≤ speed < 56 | 0.53% | 16.66% | 12.52% | 5.72% | 15.42% | 20.72% | 4.24% | 6.60% |
| 9 | 56 ≤ speed < 64 | 1.94% | 23.49% | 12.83% | 2.68% | 6.08% | 10.06% | 2.56% | 10.90% |
| 10 | 64 ≤ speed < 72 | 5.05% | 16.30% | 10.51% | 1.90% | 13.21% | 3.84% | 1.45% | 5.30% |
| 11 | 72 ≤ speed < 80 | 11.70% | 10.19% | 12.69% | 0.74% | 9.98% | 2.85% | 0.53% | 5.30% |
| 12 | 80 ≤ speed < 89 | 28.73% | 4.30% | 12.21% | 1.04% | 6.75% | 2.21% | 0.65% | 4.59% |
| 13 | 89 ≤ speed < 97 | 34.24% | 0.51% | 1.82% | 0.15% | 1.90% | 0.62% | 0.08% | 0.00% |
| 14 | 97 ≤ speed < 105 | 14.99% | 0.00% | 0.02% | 0.00% | 0.04% | 0.03% | 0.00% | 0.30% |
| 15 | 105 ≤ speed < 113 | 0.18% | 0.00% | 0.00% | 0.00% | 0.00% | 0.00% | 0.00% | 0.00% |
| 16 | 113 ≤ speed < 121 | 0.01% | 0.00% | 0.00% | 0.00% | 0.00% | 0.00% | 0.00% | 0.00% |

**Appendix F**: Single average speed for each road type

| Speed bins | Speed (km/h) | Road Types 101 | 102 | 103 | 104 | 105 | 106 | 107 | 108 |
|---|---|---|---|---|---|---|---|---|---|
| 1 | speed < 4 | 0% | 0% | 0% | 0% | 0% | 0% | 0% | 0% |
| 2 | 4 ≤ speed < 8 | 0% | 0% | 0% | 0% | 0% | 0% | 0% | 0% |
| 3 | 8 ≤ speed < 16 | 0% | 0% | 0% | 0% | 0% | 0% | 0% | 0% |
| 4 | 16 ≤ speed < 24 | 0% | 0% | 0% | 0% | 0% | 0% | 0% | 0% |
| 5 | 24 ≤ speed < 32 | 0% | 0% | 0% | 0% | 0% | 0% | 100% | 0% |
| 6 | 32 ≤ speed < 40 | 0% | 0% | 0% | 100% | 0% | 0% | 0% | 0% |
| 7 | 40 ≤ speed < 48 | 0% | 0% | 0% | 0% | 0% | 100% | 0% | 100% |
| 8 | 48 ≤ speed < 56 | 0% | 0% | 100% | 0% | 100% | 0% | 0% | 0% |
| 9 | 56 ≤ speed < 64 | 0% | 100% | 0% | 0% | 0% | 0% | 0% | 0% |
| 10 | 64 ≤ speed < 72 | 0% | 0% | 0% | 0% | 0% | 0% | 0% | 0% |
| 11 | 72 ≤ speed < 80 | 0% | 0% | 0% | 0% | 0% | 0% | 0% | 0% |
| 12 | 80 ≤ speed < 89 | 100% | 0% | 0% | 0% | 0% | 0% | 0% | 0% |
| 13 | 89 ≤ speed < 97 | 0% | 0% | 0% | 0% | 0% | 0% | 0% | 0% |
| 14 | 97 ≤ speed < 105 | 0% | 0% | 0% | 0% | 0% | 0% | 0% | 0% |
| 15 | 105 ≤ speed < 113 | 0% | 0% | 0% | 0% | 0% | 0% | 0% | 0% |
| 16 | 113 ≤ speed < 121 | 0% | 0% | 0% | 0% | 0% | 0% | 0% | 0% |

1087   **Appendix G**:

1088

1089   The annual emission rate between original road type ASD, adjusted road type ASD, and CAPSS
1090   result for 2015

| Gg/year | CO | NOx | SOx | PM10 | PM2.5 | VOC | NH3 |
|---|---|---|---|---|---|---|---|
| CARS data 2015 org ASD | 269.3 | 258.4 | 0.2 | 9.5 | 8.8 | 38.9 | 12.4 |
| CARS data 2015 adj ASD | 373.9 | 301.8 | 0.2 | 11.0 | 10.1 | 61.2 | 12.5 |
| CAPSS 2015 | 245.5 | 369.6 | 0.2 | 9.6 | 8.8 | 46.1 | 10.1 |

1091

1092

1093

1094   **Appendix H**:

1095

1096   CARS model input data summary table

| Input data type | Parameters | Variable Name in CARS | File format |
|---|---|---|---|
| **Human activity data of each vehicle** | Fuel, vehicle, type, daily VKT, region code, manufacture data | activity_file | csv |
| **Emission factor table** | Vehicle, engine, fuel, SCC ,Pollutant, year, temperature, v,a,b,c,d,f,k | Emis_factor_list | csv |
| **Link level Shape file** | Link ID, region code, region name,  road rank, speed, VKT, Link length, geometry | Link_shape | shape file |
| **County Shape File** | Region code, region name | county_shape | shape file |
| **Average speed distribution table** | Speed bins, the distribution of each road type | avg_SPD_Dist_file | csv |
| **road restriction table** | Vehicle, engine, fuel, road types | road_restriction | csv |
| **Vehicle deterioration table** | Vehicle, engine, SCC, fuel, Pollutant, Manufacture date | Deterioration_list | csv |
| **Control strategy factors table** | Vehicle, engine, fuel, year, data, region code, control factor | control_list | csv |
| **Model domain description** | Projection method name, parameters for prjection method, domain name, bottum left coner X and Y, grid cell size, numbers of grid cell in X, Y, and Z-axis | gridfile_name | text file in griddesc format |
| **Temporal profile tables** | Profile reference number, Year to Monthly profile (12 columns) | temporal _monthly_file | csv |
| | Profile reference number, week to daily profile (7 columns) | temporal _week_file | csv |

| | Profile reference number, week day to hourly profile (24 columns) | temporal_weekday_file | csv |
|---|---|---|---|
| | Profile reference number, weekend day to hourly profile (24 columns) | temporal_weekend_file | csv |
| | Vehicle, types, fuel, road type, month reference number, week reference number, weekday reference number, weekend reference number | temporal_CrossRef | csv |
| **Chemical profile table** | Species code, species name, target species name, fraction, molecular weight, | Chemical_profile | txt or csv |
| | Vehicle, engine, fuel, species reference codes | speciation_CrossRef | csv |

1097
1098